FUNCTIONALIZATION OF CELLULOSE NANOFIBRILS AND THEIR APPLICATIONS AS NOVEL MATERIALS

by

Jake Wilkinson

A Thesis

Submitted to the Faculty of Purdue University

In Partial Fulfillment of the Requirements for the degree of

Master of Science

Department of Chemistry

West Lafayette, Indiana

May 2022

THE PURDUE UNIVERSITY GRADUATE SCHOOL

STATEMENT OF COMMITTEE APPROVAL

Dr. Alexander Wei

Department of Chemistry

Dr. Jianguo Mei

Department of Chemistry

Dr. Jeffery Youngblood

Department of Materials Engineering

Approved by:

Dr. Christine Hrycyna

Dedicated to Abbey and Poppy

ACKNOWLEDGMENTS

I would like to thank my predecessors Miran Malvan, and Taehoo Chang for their excellent work on laying the groundwork for this project and for their many intellectual contributions. Rudan Feng also deserves particular mention for teaching me much about the various procedures when I was still new to the project. Yuichiro Watanabe and Benjamin Washer are to be greatly thanked as well for their endless patience and abundant willingness to help me find equipment around the lab and to teach me new skills. Indeed, the entire Wei lab has my thanks for welcoming me into their arms and for lending me assistance when I needed it.

TABLE OF CONTENTS

LIST OF TABLES 7
LIST OF FIGURES 8
LIST OF ABBREVIATIONS 9
ABSTRACT 10
CHAPTER 1. PROPERTIES, SIGNIFICANCE, AND APPLICATIONS OF CELLULOSE NANOFIBRILS 11
1.1 Introduction to the Principles of Green Chemistry and Cellulose 11
1.2 Cellulose Purification and the Differences Between Cellulose Nanofibrils (CNF) and Cellulose Nanocrystals (CNC) 14
1.3 Surface Modification of Cellulose Nanofibrils and Mechanochemistry 15
1.4 Preparation of Oleyl-CNF and Degree of Substitution Analysis 20
1.5 Oleyl-CNF as a Superhydrophobic Material 22
CHAPTER 2. PROCESS OPTIMIZATION FOR THE PREPARATION OF ESTERIFIED CELLULOSE NANOFIBERS 25
2.1 Reasons for Optimizing eCNF Synthesis 25
2.2 Improvements to lyophilization 27
2.3 Changes in Esterification Procedure and Attempts to Modify the Aerogel Grinding Process 29
2.4 Changes to eCNF Workup and Reaction Scale 32
2.5 Effect of CNF Refinement on Degree of Substitution 33
CHAPTER 3. CHEMISTRIES FOR THE CROSSLINKING OF OLEYL- CELLULOSE NANOFIBERS 36
3.1 Why Reinforcement of Esterified CNF-based Materials is Necessary 36
3.2 Development of Crosslinking Chemistry with Methyl Oleate 37
3.3 Dithiols in Thiol-Ene “Click” Chemistry 39
3.4 Epoxide Ring Opening for Crosslinking of Oleyl CNF 40
CHAPTER 4. SPRAY COATING APPLICATIONS OF OLEYL CNF MATERIALS 46
4.1 Optimization of Spray-coating Procedure 46
4.2 Applications of Spray-coated Oleyl-CNF 47

CONCLUSION 50
REFERENCES 51

LIST OF TABLES

Table 1.1. The 12 guiding principles of Green Chemistry and their adages[4] 12

Table 2.1. Original and revised procedures for the conversion of aqueous CNF slurries into esterified CNFs. 26

Table 2.2. Degree of substitution (DOS) values for eCNF samples prepared from 3 wt% CNF (blue) and 4.5 wt% CNF (green).[a] 28

Table 2.3. Degree of substitution (DOS) and Contact Angle (CA) values for eCNF samples prepared using CNF ground without solvent (blue) and EtOH-ground CNF (green and red).[a] ... 31

Table 2.4. Ethanol-assisted ball milling as an alternative workup for eCNF synthesis.[a] 33

Table 2.5. DOS and CA values of eCNFs prepared from CNFs with different refinement levels. 35

Table 4.1. Static contact angle and sliding angles of oleyl-CNF coatings on various substrates. 47

LIST OF FIGURES

Figure 1.1. Molecular structure of cellulose, with hydrogen bonding between polymer chains.[4] The repeating unit (anhydrocellobiose) is shown at right. 13

Figure 1.2. Acid hydrolysis of CNFs into CNCs and their relative dimensions.[4] 15

Figure 1.3. (A) Planetary mill, (B) Tumbling (horizontal) ball mill, (C) vibrational mixer, (D) twin-screw extruder.[4] 17

Figure 2.1. SEM images of CNF aerogels (left and middle columns) and eCNF wafers (right most column). 29

Figure 2.2. Effects of LAG on CNF aerogels. Minimal addition of EtOH improves homogeneity and reduces static buildup, while excessive amounts cause problematic clumping. 30

Figure 2.3. SEM images of "90% refined" and "100% refined" oleyl-CNF, with the former showing the presence of microfibers. 34

Figure 3.1. Cartoon depicting the introduction of crosslinks between free polymer chains, resulting in a covalent network. 36

Figure 3.2. Crosslinks between two oleyl side chains or an oleyl side chain with CNF hydroxyls. 37

Figure 3.3. Side chain for methyl oleate (R = CH_3) and oleyl-CNF 38

Figure 3.4. (A) Oleyl-CNF after mechanical grinding, demonstrating the difficulty of pulverizing dry samples. (B) Oleyl-CNF stored as a slurry in EtOH. 38

Figure 3.5. AIBN-mediated addition of thiols to methyl oleate (thiol-ene reaction).[53] 40

Figure 3.6. Various reactions attempted (Paths 1–3) and proposed reaction (Path 4) for the epoxidation of methyl oleate, a molecular analog of oleyl-CNF. 41

Figure 3.7. ^{1}H NMR of methyl epoxyoleate (400 MHz, $CDCl_3$). 41

Figure 3.8. Crystal structure of the urea–hydrogen peroxide (UHP) complex.[73] 42

Figure 3.9. ^{1}H NMR (400 MHz, $CDCl_3$) of methyl epoxyoleate synthesized by MTO-catalyzed UHP epoxidation under mechanochemical conditions. 44

Figure 4.1. Commercially available airbrush used for eCNF spray coating. 46

Figure 4.2. A cardboard box sprayed with oleyl-CNF becomes non-wetting on the outer surfaces, although forced submersion in water leads to leakage through the seams. 48

Figure 4.3. Printer paper sprayed in the center with oleyl CNF can still be printed on and will maintain its non-wetting character. 49

Figure 4.4. Newspaper spray-coated with Oleyl-CNF can be folded into an origami boat that is non-wetting and remains afloat even after several hours 49

LIST OF ABBREVIATIONS

CA	-	Contact Angle
CDI	-	Carbonyldiimidazole
CNC	-	Cellulose Nanocrystal
CNF	-	Cellulose Nanofibril
DCA	-	Dynamic Contact Angle
DOS	-	Degree of Substitution
eCNF	-	Esterified Cellulose Nanofibril
LAG	-	Liquid Assisted Grinding
mCPBA	-	m-Chloroperoxybenzoic Acid
MTO	-	Methyltrioxorhenium
OA	-	Oleic Acid
SHP	-	Superhydrophobic
TBA	-	t-Butyl Alcohol
TsOH	-	p-Toluenesulfonic acid
UHP	-	Urea Hydrogen Peroxide
YSZ	-	Yttrium-Stabilized Zirconia

ABSTRACT

Cellulose-based materials have been attracting significant attention in recent years for their potential as renewable and biodegradable materials. Cellulose nanofibrils (CNFs) in particular are readily attainable from woody biomass in high purity and without harsh chemical processes. These CNFs can undergo chemical surface modifications after a simple workup, imbuing them with new attributes that differ from their naturally paper-like structure and properties. In this research, CNFs are modified with oleic acid—another common biomass found in high concentrations in some vegetable oils—which transforms the naturally hydrophilic cellulose into a superhydrophobic material. This transformation can be carried out using solventless mechanochemistry and worked up in ethanol, supporting a green process from start to finish.

Since cellulose contains many free, exposed hydroxyl groups, carboxylic acids can be condensed onto exposed hydroxyls to form esters. In this research, we focus specifically on the oleic acid moiety because its internal alkene has potential for further reactivity. Here we explore methods to introduce crosslinks into esterified CNF (eCNF) for structural and mechanical reinforcement between fibrils. Several methods are attempted, including methods involving thiol-ene chemistry and epoxide ring opening.

Additionally, efforts have been made to develop a method to disperse eCNF materials in ethyl acetate for deposition by spray coating. Dispersions of eCNF in ethyl acetate are sufficiently stable to enable deposition using simple airbrushing tools. The eCNF coatings are homogenous, superhydrophobic, and have good adhesion to a wide variety of surfaces.

CHAPTER 1. PROPERTIES, SIGNIFICANCE, AND APPLICATIONS OF CELLULOSE NANOFIBRILS

1.1 Introduction to the Principles of Green Chemistry and Cellulose

The scientific community has become more sensitive to the negative environmental impacts of the chemistry that our economy relies on, and is thus turning its attention toward the development of new reactions, materials, and methods with a gentler impact on the planet. Three decades ago, problems such as increasing CO_2 levels responsible for the greenhouse effect, irresponsibly dumped plastic waste resulting in the Great Pacific Garbage Patch, and the hundreds of expensive-to-clean Superfund sites across the United States inspired the US Congress to pass the Pollution Prevention Act of 1990.[1] This act set a new approach to reduce pollution through improved manufacturing and design rather than by post-use treatment or waste disposal. However, without a set of guidelines, developing less harmful chemical reactions and processes remained an opaque ideal. In 1998, Paul Anastas and John Warner helped to clarify the goals of "green chemistry" by introducing the 12 Principles of Green Chemistry (Table 1.1).[2] As a result, many industrial research and development efforts have been guided by one or more of these principles.[3]

Table 1.1. The 12 guiding principles of Green Chemistry and their adages[4]

1. Waste Prevention	The prevention of waste is better than containment
2. Atom Economy	Reduce waste not just on the macro level, but also the molecular level
3. Less Hazardous Synthesis	Choose shorter and safer routes with the environment and scientist in mind
4. Design Benign Chemicals	Reagents should be designed to be less toxic
5. Benign Solvents & Auxiliaries	Always try to avoid solvents, but if needed judicious selection of a green solvent to be used at a minimum amount
6. Design for Energy Efficiency	If possible, avoid high or low temperature and pressure conditions. Ambient reactions are best
7. Use of Renewable Feedstock	When possible (availability and cost) plant based raw materials should be chosen over petroleum based
8. Reduce Derivatives	Simplify synthesis as much as possible by avoiding unnecessary steps (e.g. no protecting groups)
9. Catalytic over Stoichiometric	When possible, always choose catalytic over stoichiometric conditions
10. Design for Degradation	Plan ahead for choosing reagents and conditions with biodegradable byproducts
11. Real Time Analysis of Pollution	Monitor reactions to minimize or remove hazardous byproducts before build-up
12. Inherently Benign Chemistry for Accident Prevention	An inherently safer strategy that may give moderate yield is better than a high yielding hazardous route

Cellulose is Earth's most abundant biopolymer and is the major component in trees and many woody plants, making up around 40% of all terrestrial biomass.[5] This abundance, coupled with the rapid growth and renewal of cellulose-rich plants, makes cellulose one of the most biorenewable materials on Earth. Furthermore, nature has an extensive capacity to break down cellulose and recycle it for other uses, meaning that it is also a highly biodegradable material. This combination of intrinsic biorenewability and biodegradability makes cellulose an ideal feedstock for the development of new sustainable, or "green" materials.

On a molecular level, cellulose is a simple polysaccharide consisting of linear chains of 1,4-linked glucose units, with a degree of polymerization in the tens of thousands.[6] Each glucose unit in cellulose (or anhydroglucose, FW $C_6H_{10}O_5$) contains three hydroxyl groups available for hydrogen bonding whose orientations alternate by 180° every other unit, meaning that the repeating unit is best defined as a 1,4-linked glucose dimer (cellobiose). The regular structure of the cellulose polymer permits hydrogen bonding to play a defining role in its higher-order structure

(Figure 1.1). Aligned chains of cellulose assemble into nanocrystalline segments separated by amorphous regions, which aggregate further into bundled fibrils. The crystalline and amorphous regions of these cellulose nanofibers have different physical and mechanical properties, and also degrade at different rates when exposed to acidic conditions.[4]

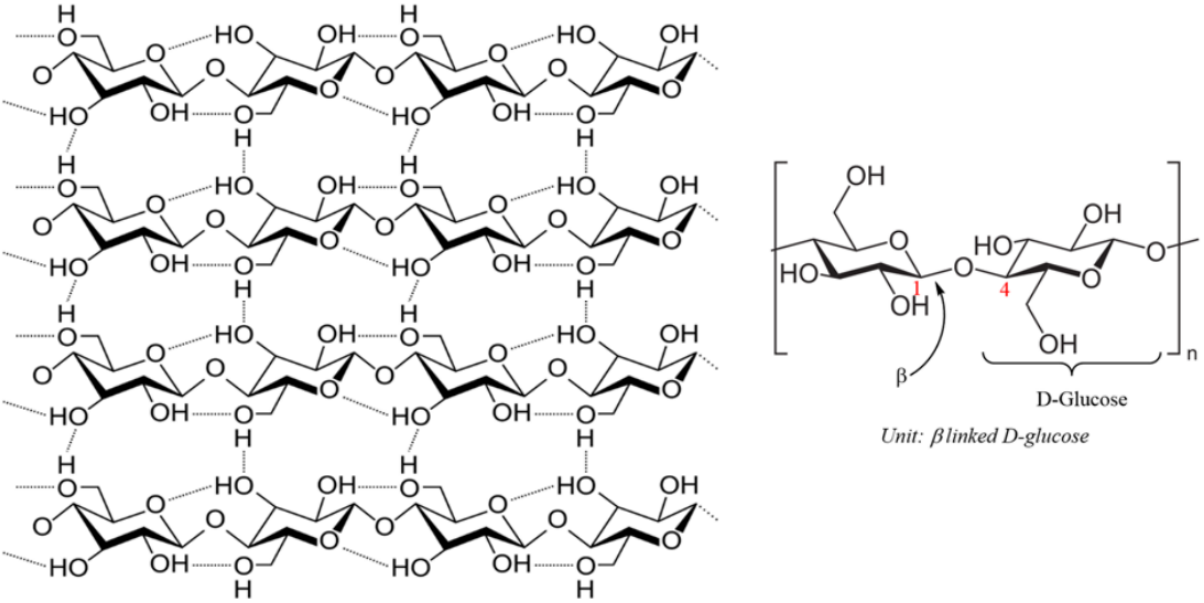

Figure 1.1. Molecular structure of cellulose, with hydrogen bonding between polymer chains.[4] The repeating unit (anhydrocellobiose) is shown at right.

Cellulose may be obtained from a number of sources beyond plant matter. Several bacteria are known to produce highly crystalline cellulose nanofibers, including Acetobacter,[7] Alcaligenes,[8] Pseudomonas,[9] and Sarcina.[10] A handful of marine organisms such as tunicates are also known to produce cellulose.[11] However, maintaining these sources of cellulose is more burdensome or expensive than simply growing plants and harvesting their woody components.

One long-term goal of cellulose research is to develop materials that can serve as sustainable alternatives to cheap and abundant plastics, particularly single-use plastics used in packaging. As such, the scale of production and the various costs associated with the product's lifecycle represent two essential pillars of this research. While cellulose can be obtained from numerous sources and in varying quality, wood-derived cellulose stands out above the others for its high abundance, low cost, and renewability. For these reasons, wood is the primary source of cellulose used in this research dissertation.

1.2 Cellulose Purification and the Differences Between Cellulose Nanofibrils (CNF) and Cellulose Nanocrystals (CNC)

In order to obtain pure cellulose from wood and plant matter, other forms of biomass must first be removed. The most significant non-cellulosic biomass present in woody sources are lignin and hemicellulose.[12] The segregation process consists of mechanical grinding followed by chemical treatments to bleach and delignify the wood pulp, followed by treatment with moderate acid such as H_3PO_4.[13] The resulting cellulose exists as an aqueous slurry and takes the form of aggregated fibers consisting of crystalline and amorphous regions. These bundled fibers typically measure up to 3 mm in length and up to 50 μm in width. Cellulose nanofibers (CNF) can be generated by further defibrillation via a variety of mechanical methods, including grinding, ball milling, sonication, and high-pressure homogenization.[14] The resulting CNFs are generally a few micrometers in length and can be refined down to 5–20 nm in width.[4]

Treatment of CNFs with a stronger acid will degrade the amorphous regions to produce cellulose nanocrystals (CNC), with 54–88% of the material comprised of highly crystalline domains (Figure 1.1).[15,16] While CNCs are structurally more homogeneous, they are also more expensive and less "green" as a biorenewable feedstock because of the additional treatment with strong acids. With this in mind, CNFs stand out as the greener, more economically viable material, if challenges to chemical processing can be overcome.

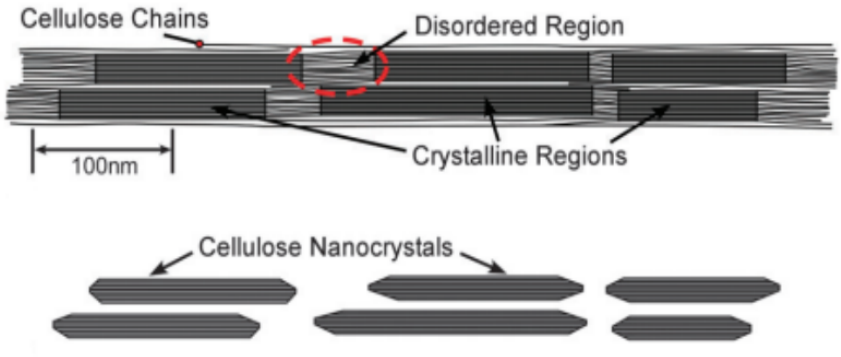

Type	Length (µm)	Width (µm)	Height (nm)	Crystallinity %
CNF	0.5 – 2	4 – 20	4 – 20	---
CNC	0.05 – 0.5	3 – 5	3 – 5	54 – 88

Figure 1.2. Acid hydrolysis of CNFs into CNCs and their relative dimensions.[4]

Wood-based nanocellulose feedstocks are offered commercially as slurries suspended in an aqueous medium (3 wt%). CNF slurries are white and opaque, and maintain their opacity when cast and dried as thin films. The lack of transparency is due to the diameter of aggregated fibers which is on the order of microns, which cause significant light scattering.[18] This opacity can be reduced significantly, however, by applying mechanical or vacuum pressure to remove air and close interstitial gaps.[19]

1.3 Surface Modification of Cellulose Nanofibrils and Mechanochemistry

The exposed hydroxyl groups on CNF surfaces provide excellent targets for chemical modification. Ample research has demonstrated that these hydroxyls will participate in diverse reactions to form esters, amides, carbamates, and ethers.[4] In each case the modified CNFs are imbued with new surface properties. CNF surface modification can reduce agglomeration,[20] increase dispersion stability in various solvents,[21] or facilitate blending with polymers such as polyethylene[17,22] and polylactic acid[23] or with conductive carbon nanotubes[24] to create hybrid

nanomaterials. In this dissertation, oleic acid (OA) is grafted onto the surfaces of CNFs to create a superhydrophobic material.

Generally, surface modifications take place in the presence of an organic solvent; however, these are considered auxiliary and can account for up to 90% of the waste produced in synthetic processes.[25] From the perspective of sustainability, the ideal reaction would minimize the use of organic solvent or eliminate it altogether. One method for performing chemical transformations with minimum solvent is mechanochemistry, a method that dates back thousands of years to simple grinding with a mortar and pestle.[26] While grinding by hand still has its place in the modern chemistry lab, mechanochemical methods have evolved to remove the manual aspect of this process with greatly improved efficiency.

While chemists often apply sources of energy such as heat, electricity, or electromagnetic radiation to drive reactions forward, the use of mechanical force to introduce chemical energy is often overlooked. Two of the most common mechanochemical processes used today involve ball milling using hard materials such as steel or ceramic media, or shear mixing by twin-screw extrusion in which the reaction media is forced together with high pressure. The ball-milling method relies on the frequent collision between hard spheres inside a milling chamber that undergoes planetary rotation and high-frequency vibrations, or is placed on a pair of horizontally rotating cylinders (Figure 1.3).

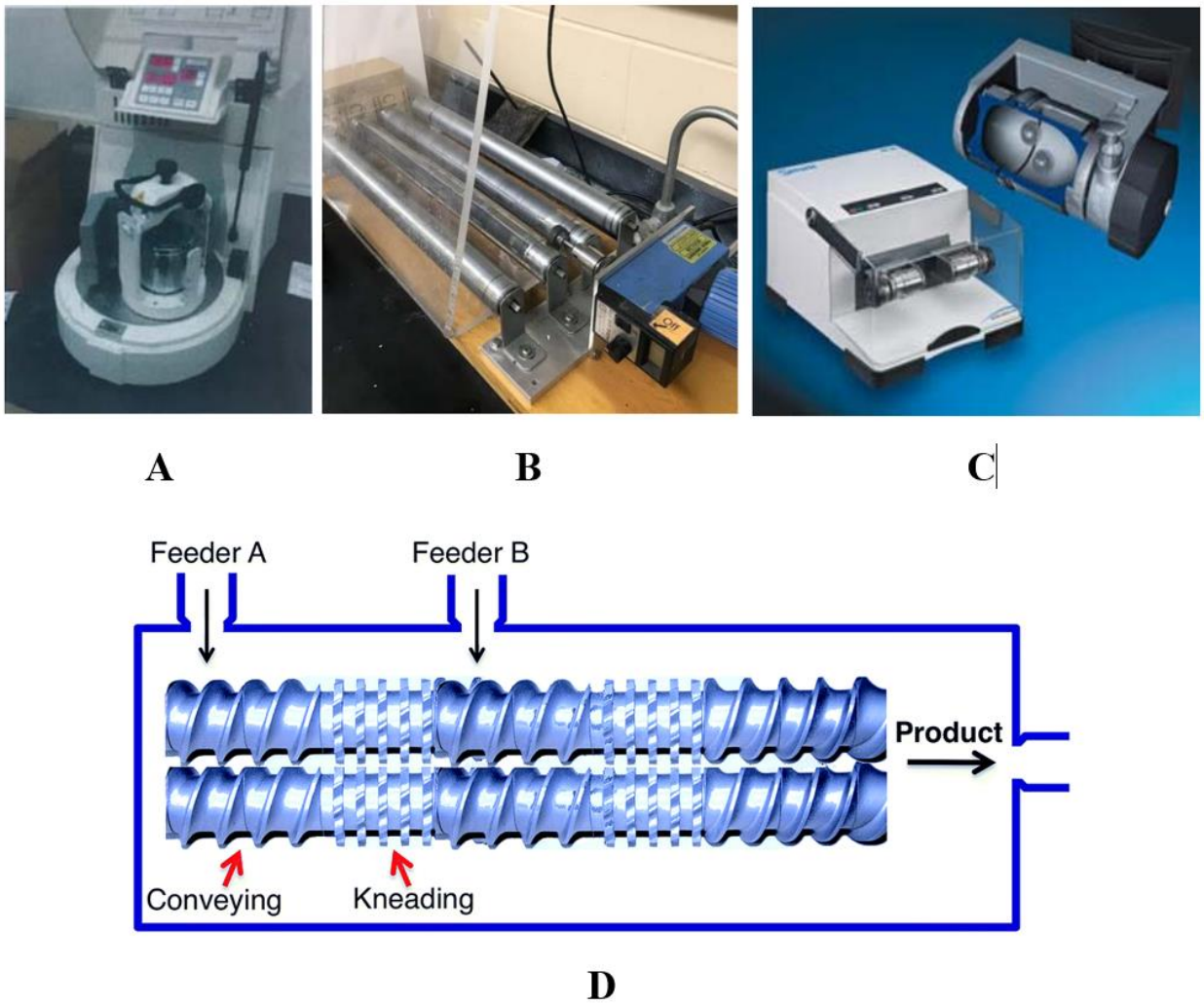

Figure 1.3. (A) Planetary mill, (B) Tumbling (horizontal) ball mill, (C) vibrational mixer, (D) twin-screw extruder.[4]

The mechanisms by which mechanochemistry operates have not yet been fully elucidated and remain an active area of research. Resultingly, reaction optimizations rely chiefly on experimentation.[4] It is now established that mechanochemistry can unlock unique reaction pathways that can generate products or product ratios that differ from those attainable via pathways that involve solvents.[27,28] One concept used to explain novel effects of mechanochemistry is the "hot-spot" theory, which asserts that the heat generated by each ball-to-ball or ball-to-container collision is enough to drive a reaction forward.[29] Reactants trapped between hard surfaces experience localized heating, in contrast to traditional methods that raise the temperature of the entire system in order to shift a reaction equilibrium. The "hot-spot" theory is consistent with the empirical evidence that the mass and density of the milling media is important for optimizing a

mechanochemical process, but stops short of the notion that collisions generate a transient plasmatic state, as some older (and now less popular) theories have asserted.[30]

Previous work in the Wei research group has demonstrated that CNFs react readily with a variety of carboxylic acids in the presence of carbonyldiimidazole (CDI) under horizontal ball milling conditions.[4] While some mechanochemical reactions call for a small amount of solvent to aid the mixing of otherwise dry compounds, a practice known as liquid-assisted grinding (LAG), the reactions explored in this work do not need any extra solvent, due to the liquid state of OA at ambient temperature. For example, the reaction between neat OA and finely powdered CDI produces a viscous slurry, which is then blended with granulated CNF into a dough-like mixture. The replacement of liquid-based reactions with mechanochemistry allows us to eliminate the use of organic solvents, Tenet #5 of the 12 Principles of Green Chemistry. Indeed, nearly all of the Principles of Green Chemistry are satisfied by the chemistry employed in this research.

At present, esterified CNFs (eCNFs) are held together by noncovalent forces and are thus mechanically fragile and easily torn. A possible solution to this problem is to introduce functional groups that can be crosslinked covalently. Crosslinking is widely used to reinforce the mechanical strength of polymeric materials and is commonly employed in the strengthening of elastomers.[47] Vulcanization, one of the first methods developed for the toughening of rubber, involves the insertion of polysulfur crosslinks between alkenes (Figure 1.4).[48] Because oleyl-CNF also contains alkenes, it is possible to adapt such a process directly toward strengthening CNF-based materials. Vulcanization does have some drawbacks however, such as sample discoloration, odor, and leaching.[49] A variant to this approach utilizes dithiols rather than elemental sulfur; although still malodorous, they can be used in smaller amounts and do not exhibit significant leaching and discoloration problems.[50] However, many reactions that have been developed for thiol-ene "click chemistry" rely on photoinitiation, which is problematic for CNF-based materials that are opaque and prevent the deep penetration of UV or visible light.[50-54]

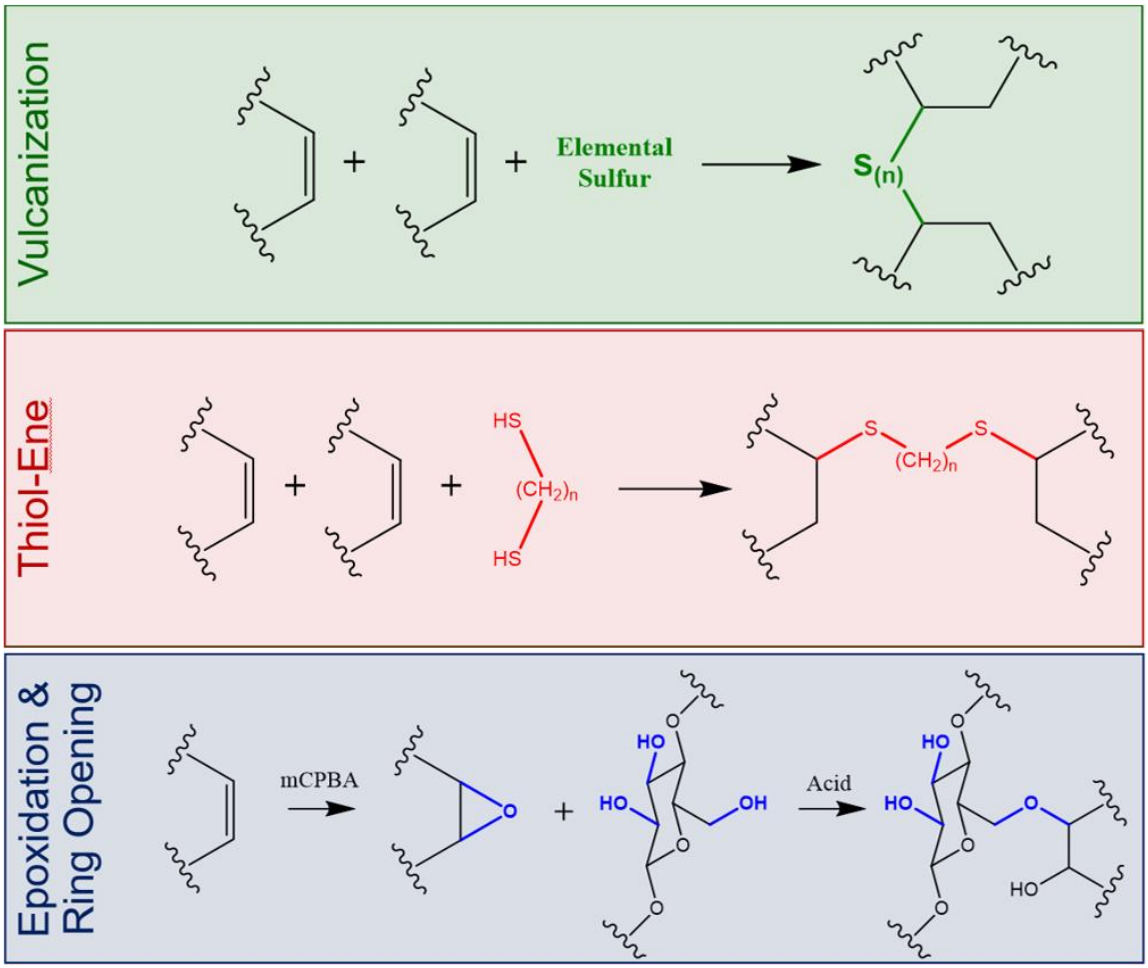

Figure 1.4. Reaction pathways for crosslinking chemistries with potential application to esterified CNFs (eCNFs).

Another approach to crosslinking involves alkene epoxidation followed by acid-catalyzed ring opening using diols or polyols (Figure 1.4). In this method, the alkene is converted into an epoxide which can then react with exposed CNF hydroxyls that were not esterified in the preceding mechanochemical reaction with OA. As will be discussed in Chapter 2, a typical DOS value achieved through CNF esterification with OA is around 0.2, which is well below the theoretical limit proposed by other researchers,[31] so it is reasonable to consider the direct crosslinking between CNF hydroxyls and epoxidized oleate groups. This approach will be discussed in greater detail in Chapter 3.

1.4 Preparation of Oleyl-CNF and Degree of Substitution Analysis

The mechanochemical method of preparing eCNFs was first developed by Dr. Miran Malvan, however no efforts were made to optimize the procedure beyond reaction stoichiometry. The process of transforming aqueous CNF feedstock (purchased as a 3 wt% slurry from Forest Products Labs) into eCNFs originally took 7 days, with the most time-consuming step being the freeze-drying or lyophilization of CNFs, requiring up to 5 days. Esterification and subsequent purification and drying required another 2 days. The time needed to produce one batch of oleyl CNF was therefore a significant obstacle not only to the advancement of this project, but also to its potential for scalable production.

In order to perform efficient esterification of CNFs, the water must first be removed to avoid competing with CNF surface hydroxyls. Simply freeze-drying the CNFs, however, results in irreversible agglomeration (hornification) which lowers the CNF surface area and reduces the exposure of available hydroxyl groups.[32] As an improvement to the freeze-drying process, it was determined that adding 10 wt% of *t*-butyl alcohol (TBA) to the CNF slurry prevented fibers from aggregation during freezing and subsequent hornification during lyophilization, resulting in the formation of aerogels with high specific surface area.[4] These aerogels were typically produced using 100 g of CNF slurry in a cylindrical plastic jar, with overnight freezing followed by 4 days of lyophilization. The resulting CNF aerogel (Figure 1.5A) was then ground into smaller pieces using a coffee grinder, resulting in a fluffy powder that was amenable to mechanochemical esterification (Figure 1.5B).

Figure 1.5. (A) CNF aerogel after lyophilization with 10 wt% TBA; (B) ground CNF; (C) pad of eCNF prepared after esterification, washing, and filtration.

Setting up CNF esterifications by mechanochemistry is straightforward. In a typical reaction described by Dr. Mavlan, 1.0 g of carbonyldiimidazole (CDI) is combined with 1.75 g of OA and 11 yttrium-stabilized zirconia (YSZ) balls (1-cm spheres) in a 100-mL Nalgene bottle. This is capped and placed on a horizontal ball mill for up to several hours, with a brief break after the first 30 minutes to release the buildup of CO_2 during CDI activation. The mixture is then treated with 0.5 g of ground CNF and subjected to ball milling for at least 6 more hours. By the end of the reaction, most of the mixture forms a thick coating on the YSZ media, requiring its physical removal before proceeding to the next step. Residual material can be collected by rinsing the milling media and reaction vessel with ethanol (EtOH), which is combined with the reaction mixture in a 250-mL beaker until the final volume is 100 mL. The ethanolic mixture is then subjected to sonication for 15 minutes at 100% power using a Ti immersion probe (the energetic nature of the sonication causes the temperature to rise up to 45 °C), resulting in a mostly homogenous suspension. The esterified CNFs can be collected by vacuum filtration and rinsed with fresh EtOH, then strained until a damp pad is formed. The oleyl-CNFs are shredded and resuspended in 100 mL of fresh EtOH and sonicated for another 15 minutes, then filtered and rinsed as before. The pad of purified oleyl-CNF is then removed and dried in air for 24 hours (Figure 1.5C).

The esterification reaction can be evaluated quantitatively by estimating the degree of substitution (DOS), and qualitatively by testing its superhydrophobicity (to be discussed in further detail in Chapter 4). If water droplets do not stick to the surface and roll off with ease, the sample is considered to have passed the test. DOS analysis is based simply on the mass increase of covalently grafted substituents relative to the mass of CNF. In fact, DOS is a rough index of chain substitution; cellulose polymers in CNF do not exist in a free state but rather as aggregate fibers, and the heterogeneity in fiber diameter complicates the estimation of surface hydroxyls available for esterification. Indeed, most of the hydroxyl groups in each CNF fiber are inaccessible because they are buried within the fiber.

Some approaches to calculate DOS attempt to account for differences in fiber size and length.[33] However, in our research, we applied a simple method based on relative mass changes described by the Huang group (Figure 1.6).[34] This equation uses only one constant and three variables, the constant being the molar mass of an anhydroglucose unit (162 g/mol). M_w refers to

the molar mass of the functional group being grafted (i.e., the oleyl unit), and m_1 and m_2 refer to the initial mass of CNF and final mass after modification, respectively.

$$DOS = \frac{162 \times (m_2 - m_1)}{M_W \times m_1}$$

162 = Mass of one anhydroglucose unit
M_w = Molar mass of grafted functional group
m_1 = Initial mass of CNF sample
m_2 = Final mass of CNF sample

Figure 1.6. Degree of substitution (DOS) calculation by change in mass.[34]

DOS may also be evaluated by changes in the FT-IR spectrum of an esterified CNF sample. Specifically, the appearance of a carbonyl ester stretch in oleyl-CNF at 1730–1750 cm^{-1} is quite useful, as unmodified CNF should have no absorption in that region. Three other noteworthy changes include the reduction in O–H peak intensity at 3200–3600 cm^{-1}, the increase in aliphatic C–H stretching peaks at 2950–2850 cm^{-1}, and the appearance of an alkene C–H stretching peak at 3100–3000 cm^{-1}. However, using FT-IR to determine DOS is less precise than the mass-based approach, and was generally not used in the course of this project. The use of DOS as a metric for efficiency in CNF esterification is discussed further in Chapter 2.

1.5 Oleyl-CNF as a Superhydrophobic Material

Many natural and artificial materials exhibit water-repelling properties and are considered hydrophobic. Typically, the level of "wettability" of a surface is determined using liquid contact angle (CA) and sliding angle measurements.[35] CA measurements are taken on a level surface, while sliding angle measurements describe the tilt angle needed to make a static droplet roll off the surface. If a water droplet forms a CA less than 90° on a given substrate, that surface is considered hydrophilic, while a CA greater than 90° classifies a surface as hydrophobic.[36] As hydrophobicity increases, the CA also increases and the sliding angle often decreases, although the latter can be highly dependent on surface defects. Surfaces are classified as superhydrophobic (SHP) when water droplets form contact angles that exceed 150°.[37] Additionally, SHP surfaces are characterized by a sliding angle at or below 5°.[38] Examples of naturally occurring SHP materials include duck feathers and lotus leaves.[37]

Several characteristics are responsible for defining the wettability of a surface, and can be classified as being chemical or physical in nature.[39] Chemical wettability is driven by the surface energy between a solid and a liquid: lower surface energy increases solvophobicity. However, the chemical properties of a surface are not sufficient to achieve SHP, although some researchers have been able to achieve CAs as high as 130° on smooth surfaces.[40] Physical texture and surface roughness are also critical factors in wettability. The prevailing theory that relates surface roughness with SHP is known as the Cassie–Baxter model.[41] Their theory asserts that microscopic surface features can prevent liquids with from making perfect contact with a surface, resulting small pockets of air between surface peaks (Figure 1.7A). These pockets of trapped air exert a positive pressure on water droplets and prevent their strong adhesion to the surface.

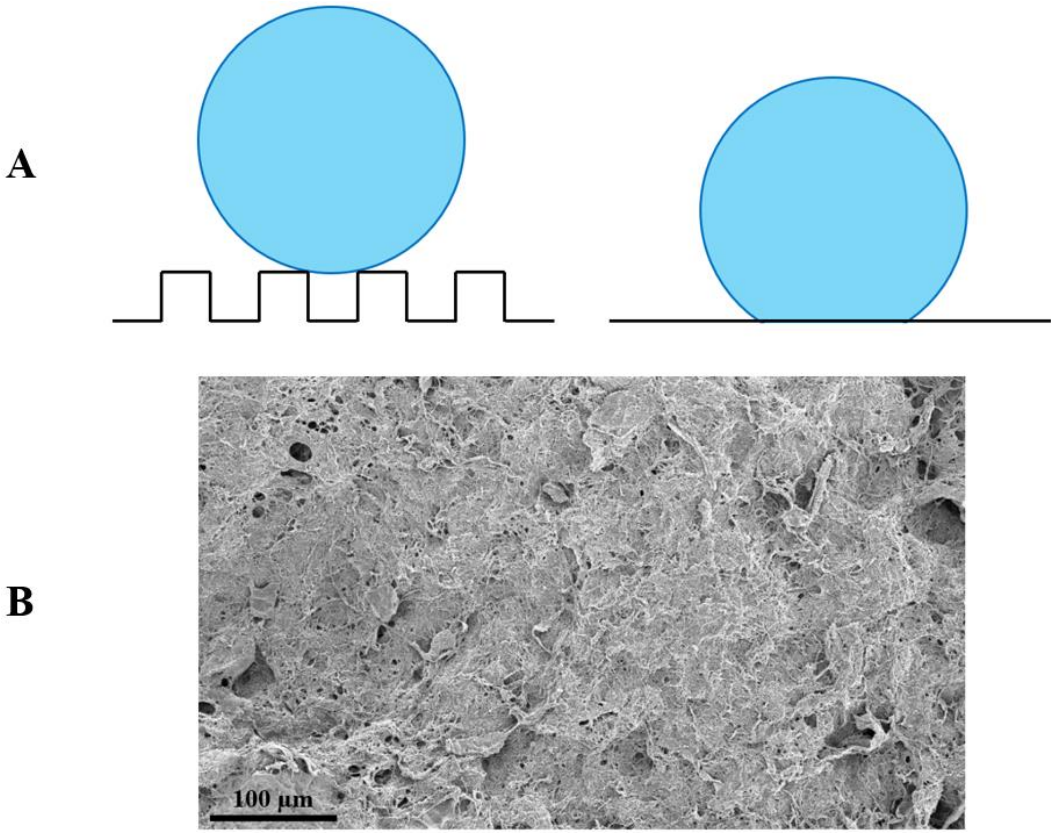

Figure 1.7. (A) Depiction of the influence of surface roughness on wettability. (B) SEM image of the surface of an esterified CNF sample, demonstrating innate surface roughness.

CNFs in their dried state have an intrinsically microtextured surface even after esterification. This is due in part to the web-like entanglement of individual fibers, which can be

resolved in SEM images (Figure 1.7B).[4] In addition to this irregular architecture, oleyl-CNFs have nonpolar fatty acid chains that impart a low surface energy. This combination of microscale roughness and low surface energy bestows the oleyl-CNF matrix with superhydrophobic properties, yielding static CAs up to 160°. Furthermore, if the surface is damaged or soiled, the hierarchical structure of CNF-based materials enables its SHP properties to be renewed by a simple and mild exfoliation—a truly unique property for synthetic SHP materials (including other CNF-based materials), many of which rely on intricate patterns of nanoscale features which are easily disturbed and non-renewable.[42-46] Developments of oleyl-CNFs as a SHP material are discussed in Chapter 4.

CHAPTER 2. PROCESS OPTIMIZATION FOR THE PREPARATION OF ESTERIFIED CELLULOSE NANOFIBERS

2.1 Reasons for Optimizing eCNF Synthesis

As discussed in Section 1.4, the original process for eCNF synthesis generally takes 7 days from start to finish. Furthermore, many of the techniques employed are not conducive to practical industrial scalability. The most problematic issue is the 4 days needed for lyophilization, which is not only time-consuming but also energy intensive—both unfavorable characteristics for the prospect of industrial scaling. In addition, workups relying on sonication are impractical on the industrial scale because the technique is used mostly on a laboratory scale.[55] Furthermore, the process of manually removing reaction product from the milling media is tedious and represents yet another step that would be benefit from workflow redesign. An ideal process should use less energy-intensive and labor-intensive means of purifying chemically modified CNFs.

In this chapter, process optimizations will be discussed that reduces the time for eCNF synthesis and purification to 3 days, while improving scalability and reducing energy and solvent waste. These optimizations can be grouped broadly into three categories: (1) improvements to the lyophilization step, (2) changes in the esterification procedure, and (3) changes to reaction workup. The major procedural changes are noted in Table 2.1 and discussed in more detail in subsequent sections. The improvements provided by these procedural changes enabled the scaleup of this reaction from 0.5 g up to 5.0 g, without any loss in product quality.

Table 2.1. Original and revised procedures for the conversion of aqueous CNF slurries into esterified CNFs.

Original Procedure[4]	Revised Procedure
Lyophilization	**Lyophilization**
• Add 10 wt% TBA to aqueous CNF slurry. • Manual stir for 5 min. • Freeze at −20 °C in wide-mouthed jar (100 cm^3). • Lyophilize for 4 days. • Grind aerogel into a granular form.	• Centrifuge aqueous CNF slurry at 3500 rpm for 30 min. Decant supernatant. • Add 10 wt% TBA. • Manually stir for 2 min, then spread evenly in a silicone mold (1 cm^3 cubes). • Freeze at −20 °C, then transfer cubes from mold onto a flat tray. • Lyophilize for 2 days. • Grind aerogel into a granular form.
Esterification	**Esterification**
• Add OA, CDI, and YSZ milling media to a 100-mL Nalgene bottle. • Ball mill for 6 hours; degas after 15 min. • Add ground CNF. • Ball mill for another 6 h, with monitoring to prevent build-up near the mouth of vessel.	• Add OA, CDI, and YSZ milling media to a 100-mL Nalgene bottle. • Ball mill for 20 min; degas after 15 min. • Add ground CNF. • Ball mill for 6 h, with monitoring to prevent build-up of solid near the mouth of vessel.
Workup	**Workup**
• Remove eCNF mixture from vessel and milling media (manually). • Rinse bottle and balls with EtOH; combine with reaction mixture. Add additional EtOH to a final volume of 200 mL/g of CNF. • Sonicate eCNF suspension with immersion probe for 15 min. • Vacuum filter suspension with rinsing until a damp cake is achieved. • Collect and shred eCNF, then resubmerge in EtOH (200 mL/g of CNF). • Sonicate eCNF suspension with immersion probe for 15 min. • Vacuum filter suspension with rinsing; continued filtration for 15 min. • Remove dried CNFs from filter paper. Air dry for 24 hours. • Weigh sample, determine DOS.	• Add EtOH (100 mL/g of CNF) to milling vessel. • Ball mill for 1 hour. • Vacuum filter suspension with rinsing until a damp cake is achieved. • Redisperse eCNF by hand mixing in EtOH (100 mL/g of CNF). • Vacuum filter suspension with rinsing until a damp cake is achieved. • Remove product from filter paper, and – store under minimal EtOH, OR – dry in air for 24 hours, then weigh sample to determine DOS.

2.2 Improvements to lyophilization

In order to reduce the time required to freeze and lyophilize a sample, several techniques were utilized. Firstly, centrifugation was attempted to dewater CNF, which is obtained as a 3 wt% slurry from Forest Products Labs (Univ. of Maine Process Development Center). This enabled us to remove a significant amount of the water (up to 50% by weight), however it was found that removing more than 33% water produced a CNF slurry that was too viscous to work with, resulting in irreversible hornification after lyophilization. A version of heated centrifugation using an instrument known as a CentriFan was also attempted, but quickly abandoned for reasons of practicality and the lower quality of CNF aerogel produced.

The dewatering step has the added benefit of reducing the amount of TBA needed for lyophilization. The quality of the CNF aerogels formed by lyophilization is crucial, as it ensures a high surface area that enables OA or other fatty acids to be grafted with a relatively high DOS. It was determined previously by Dr. Malvan that adding 10 wt% TBA to the aqueous CNF suspensions resulted in a eutectic mixture that minimized ice crystallization during freezing, with subsequent production of high-quality CNF aerogels.[4] Other additives were tested, but none were found to perform better than TBA in improving aerogel quality.

With respect to the dewatering step, a 33% reduction in water means that 33% less TBA is needed to achieve a eutectic mixture, thus contributing toward less solvent waste.[57] It is important to note that TBA is also a relatively green solvent according to the GSK Solvent Sustainability Guide,[56] which is consulted by chemists interested in the design of green processes. Just as importantly, the overall reduction in volume reduces the total work of lyophilization, as well as a reduction in lyophilization time.

By itself, the dewatering step only reduces the total lyophilization time by a few hours. We determined that lyophilization time is impacted more strongly by exposed surface area,[58] as the sublimation process becomes less efficient with sample depth. In order to increase surface area, the TBA-treated CNF slurries were spread into silicone ice cube trays (1 cm^3 volume per cube) prior to freezing. Whereas a 100 g (ca. 100 mL) sample was previously frozen and lyophilized in a single jar, the silicone mold allowed for CNFs to be frozen into much smaller unit volumes. These can be fully removed to expose all surfaces during lyophilization, thereby increasing the available surface area by nearly 10-fold. As an added benefit, samples no longer needed to be frozen overnight at –20 °C; instead, 2 hours was sufficient. This change (plus the dewatering step)

reduced the time needed to obtain lyophilized CNFs from 5 days to 2 days, with no measurable impact on the quality of subsequently prepared eCNFs (Table 2.2).

Table 2.2. Degree of substitution (DOS) values for eCNF samples prepared from 3 wt% CNF (blue) and 4.5 wt% CNF (green).[a]

Sample ID	CNF Refinement	**Concentration**	DOS
JRW 1-5a	90%	3%	0.200
JRW 1-5b	90%	3%	0.208
JRW 1-6a	100%	3%	0.121
JRW 1-6b	90%	3%	0.117
JRW 1-7a	90%	3%	0.186
JRW 1-7d	90%	3%	0.152
JRW 1-7e	100%	3%	0.160
JRW 1-24a	90%	**4.5%**	0.128
JRW 1-24b	90%	**4.5%**	0.123
JRW 1-24c	90%	**4.5%**	0.171
JRW 1-24d	100%	**4.5%**	0.135
JRW 1-24e	100%	**4.5%**	0.161
JRW 1-24f	100%	**4.5%**	0.147

[a] DOS values of 0.1–0.2 are typical and considered a good level of substitution.

The aerogels prepared using 4.5 wt% CNF slurries do not appear significantly different from those prepared using 3.0 wt% CNF when imaged by scanning electron microscopy (SEM) (Figure 2.1). Specifically, we exposed and examined the interior surfaces of these aerogels by carefully slicing a freeze-dried cube with a sharp blade. Some differences can be observed in the surface roughness of the eCNF aerogels, with the ones prepared using 4.5 wt% CNF appearing to be smoother. However, this difference does not have a significant impact on the DOS of eCNF functionalization as demonstrated in Table 2.2.

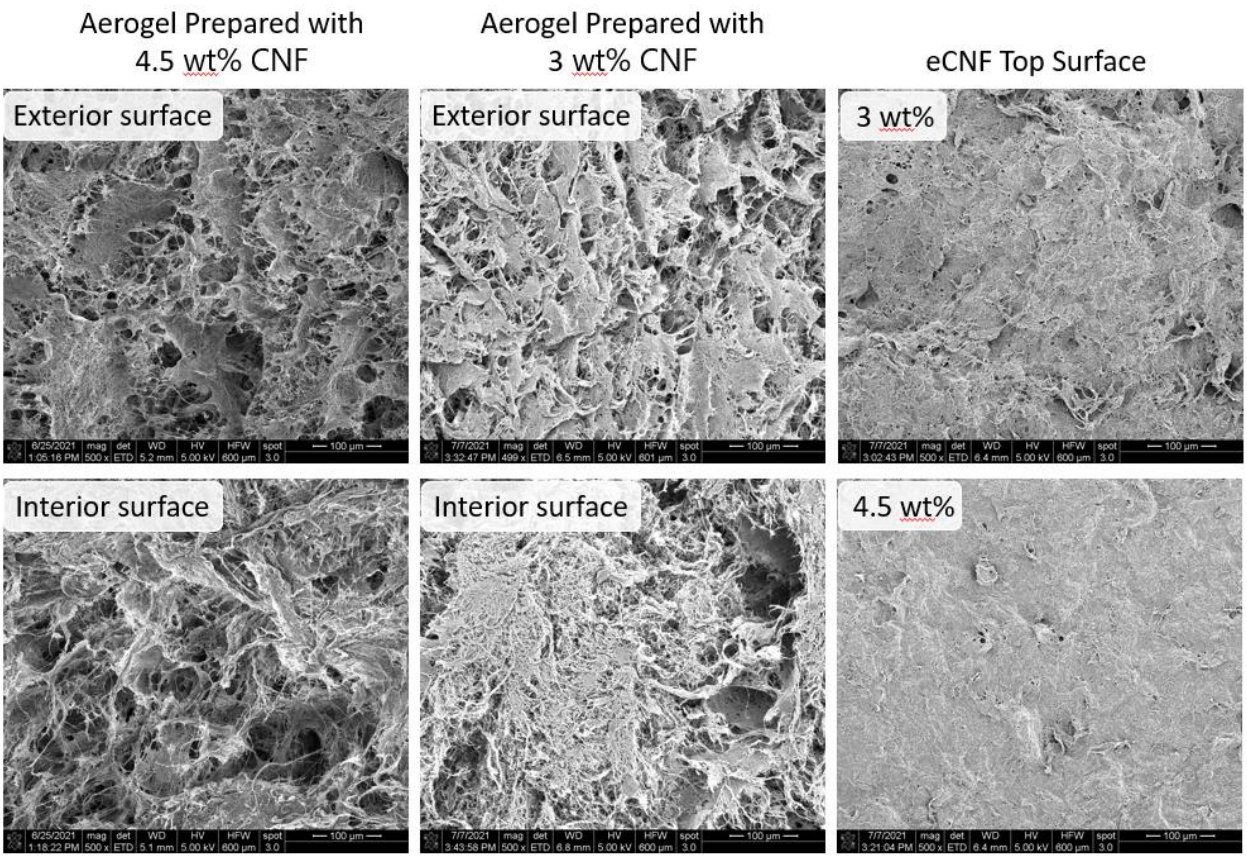

Figure 2.1. SEM images of CNF aerogels (left and middle columns) and eCNF wafers (right most column).

2.3 Changes in Esterification Procedure and Attempts to Modify the Aerogel Grinding Process

While the stoichiometry for mechanochemical CNF esterifications has been established by previous project leaders, investigations into the time required for each step in the ball milling process is more limited. Originally, the carboxylic acid activation by CDI and subsequent ball milling with granulated CNF were each performed for 24 hours. However, we determined that 6 hours is sufficient for mechanochemical esterification, and a mere 20 minutes is sufficient for OA activation by CDI. Reducing these reaction times had no significant impact on DOS values of the final product or their subsequent SHP properties (to be discussed in Chapter 3). It is noteworthy that CDI activation, CNF esterification, and the final workup steps can all be completed in a single afternoon.

We also investigated the addition of solvent to aid in the dispersion of lyophilized CNF during grinding. Our method of CNF granulation involves a plastic coffee grinder, which is prone

to electrostatic buildup and occasionally results in a heterogeneous particle mixture (Figure 2.2). The author hypothesizes that static buildup is a major contributor to heterogeneity and is a potential reason for the occasional defects in the superhydrophobic properties of the final product, which often manifests with surface wetting and droplet pinning. Static buildup presents additional handling issues as the ground CNF particles are so light that their collection is tedious and messy, and prone to sample loss.

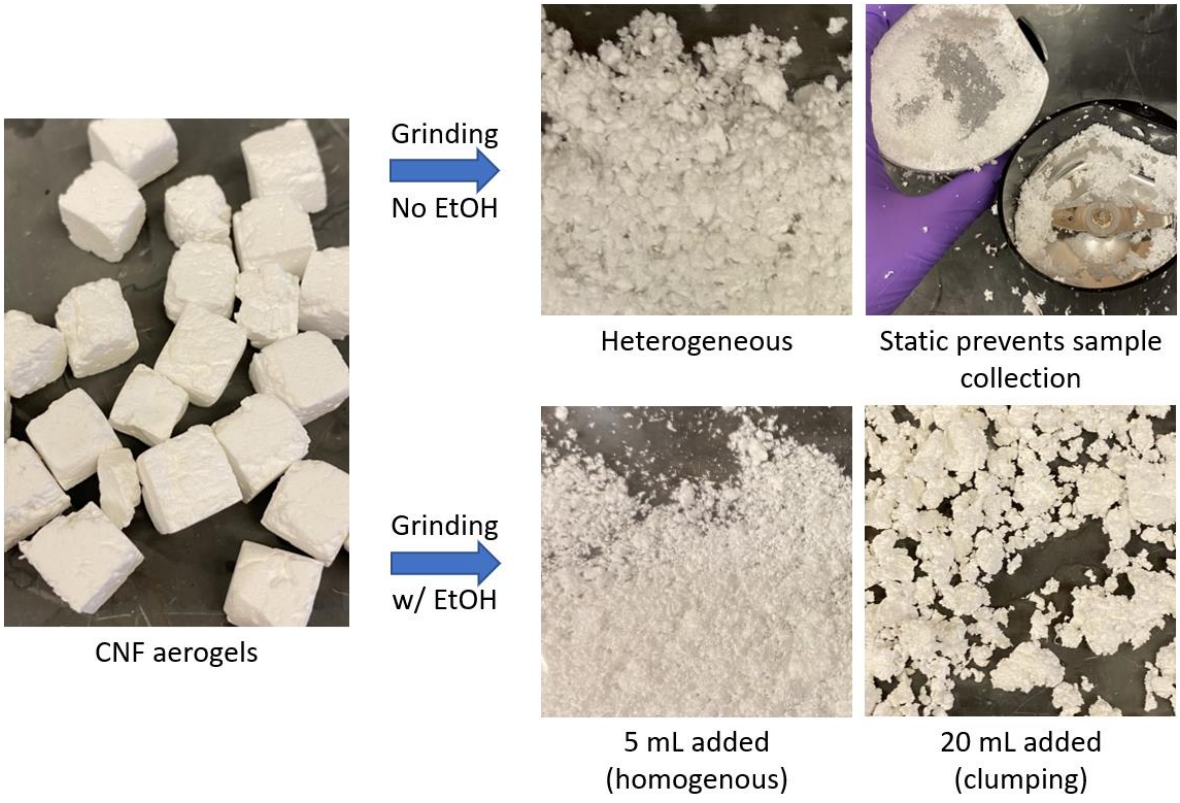

Figure 2.2. Effects of LAG on CNF aerogels. Minimal addition of EtOH improves homogeneity and reduces static buildup, while excessive amounts cause problematic clumping.

Efforts were made to combat electrostatic buildup in the coffee grinder, albeit with mixed results. Liquid-assisted grinding (LAG) was attempted to reduce the impact of electrostatic forces during grinding and to produce more homogenous particles, using ethanol given its reputation as a sustainable solvent.[56] After some optimization it was found that adding 5 mL of EtOH per gram of CNF aerogel produced particles that were visibly smaller, more homogenous, and (at least while damp) significantly less influenced by static buildup. Adding more EtOH (20 mL per gram)

resulted in clumping and was not explored further. The differences between dry and liquid-assisted grinding is presented in Figure 2.2.

While the addition of EtOH during grinding improved that part of the process, the issue remained that EtOH would likely interfere with CNF esterification because it can readily react with CDI, preventing complete activation of OA. For this reason, ethyl acetate— a solvent that should not interfere with esterification and has a relatively favorable sustainability score[56]— was tested but quickly abandoned when it became clear that the plastic coffee grinder was incompatible with the solvent. Instead, CNFs ground with EtOH were left to dry in air or vacuum over the course of 24 hours. CNF prepared in this manner were able to produce eCNF with similar DOS values as those prepared without LAG, however the hydrophobicity of the final product was inconsistent, regardless of how thoroughly the drying process was conducted (Table 2.3). We thus abandoned further attempts to modify the grinding process.

Table 2.3. Degree of substitution (DOS) and Contact Angle (CA) values for eCNF samples prepared using CNF ground without solvent (blue) and EtOH-ground CNF (green and red).[a]

Sample ID	**EtOH Grinding?**	Drying Method	DOS	CA
JRW 1-6a	No	N/A	0.123	154°
JRW 1-7e	No	N/A	0.154	153°
JRW 1-24d	No	N/A	0.135	142°
JRW 1-24e	No	N/A	0.161	157°
JRW 1-24f	No	N/A	0.147	149°
JRW 1-9e	**Yes**	Air	0.161	140°
JRW 1-9f	**Yes**	Air	0.201	142°
JRW 1-9c	**Yes**	Vacuum	0.109	143°
JRW 1-9d	**Yes**	Vacuum	0.135	109°
JRW 1-25d	**Yes**	Vacuum	0.099	140°
JRW 1-25e	**Yes**	Vacuum	0.093	142°
JRW 1-25f	**Yes**	Vacuum	0.128	134°

[a] DOS values of 0.1–0.2 are typical and considered a good level of substitution.

2.4 Changes to eCNF Workup and Reaction Scale

As mentioned previously, workups that involve sonication are not ideal on an industrial scale. Additionally, the physical removal of the reaction mixture from the milling media, which is already tedious on small scale, becomes overly burdensome for reactions on a larger scale. Fortunately, the solution to both problems is incredibly simple and intuitive: ball milling is an ideal alternative to sonication for this workup, and provides sufficient mechanical energy to aid in the redispersion of fine particles. Furthermore, adding ethanol for LAG has no negative impact on the mixture once the reaction has gone to completion, and is expected to quench any residual CDI-activated oleate.

In order to circumvent the need for sonication and physical cleaning of ball milling media, EtOH was introduced into reaction vessels immediately following mechanochemical esterification. The reaction mixture was milled until a homogenous suspension was formed, which could be achieved in just 1 hour. The eCNFs were collected by vacuum filtration, resuspended in fresh EtOH via simple hand stirring, then filtered again and dried fully in air to obtain the product mass, or retained as a ethanolic slurry for future use. This alternative workup procedure can be completed in less than 2 hours, and has no detrimental impact on the quality of the resulting eCNF in terms of mass recovery, DOS, and superhydrophobicity (Table 2.4). In order to verify that this modified workup has no detrimental effect on eCNF quality, several samples were prepared as normal, then subjected to EtOH-assisted ball milling for several hours (Table 2.4). From this screening, it is clear that the EtOH workup not only has no detectable impact on DOS, but also requires only half as much of the EtOH needed as in the workup with sonication.

Table 2.4. Ethanol-assisted ball milling as an alternative workup for eCNF synthesis.[a]

Sample ID	Amount of	Time Milled	DOS	CA
JRW 1-55a	10 mL	1 hr	0.143	150°
JRW 1-55b	15 mL	2 hr	0.156	156°
JRW 1-55c	25 mL	4 hr	0.198	149°
JRW 1-55d	35 mL	6 hr	0.142	158°
JRW 1-55e	50 mL	12 hr	0.156	159°

[a] DOS values of 0.1–0.2 are typical and considered a good level of substitution.

In addition to simplifying and streamlining the preparation of mechanochemically esterified CNF, the modified workup is very compatible with reaction scaleup. To test this, the reaction was increased in scale from 0.5 g CNF to 2.5 g and also 5.0 g. With the modified workup, these larger-scale reactions yielded eCNFs with the same or better quality as those obtained at the 0.5-g scale. We also determined that the eCNFs can be stored stably under EtOH for many weeks without apparent fiber aggregation or loss of SHP properties in the final material.

2.5 Effect of CNF Refinement on Degree of Substitution

Our source of CNFs (Forest Product Labs at the Univ. of Maine Process Development Center) provides slurries at two different levels of defibrillation. “90% refined” contains a small but significant percentage of bundled cellulose fibers with diameters on the order of several microns, whereas “100% refined” are devoid of such microfibers. Differences between 90% and 100% refined CNF can be seen in Figure 2.3, with microscale fibers clearly visible in the 90% refined sample. However, it was unknown whether refinement level might result in a discernable difference in performance between eCNF products, namely their superhydrophobic qualities. Answering this question was important to ensure that data generated from these two sources were comparable, as the Forest Product Labs no longer sells a 90% refined CNF product.

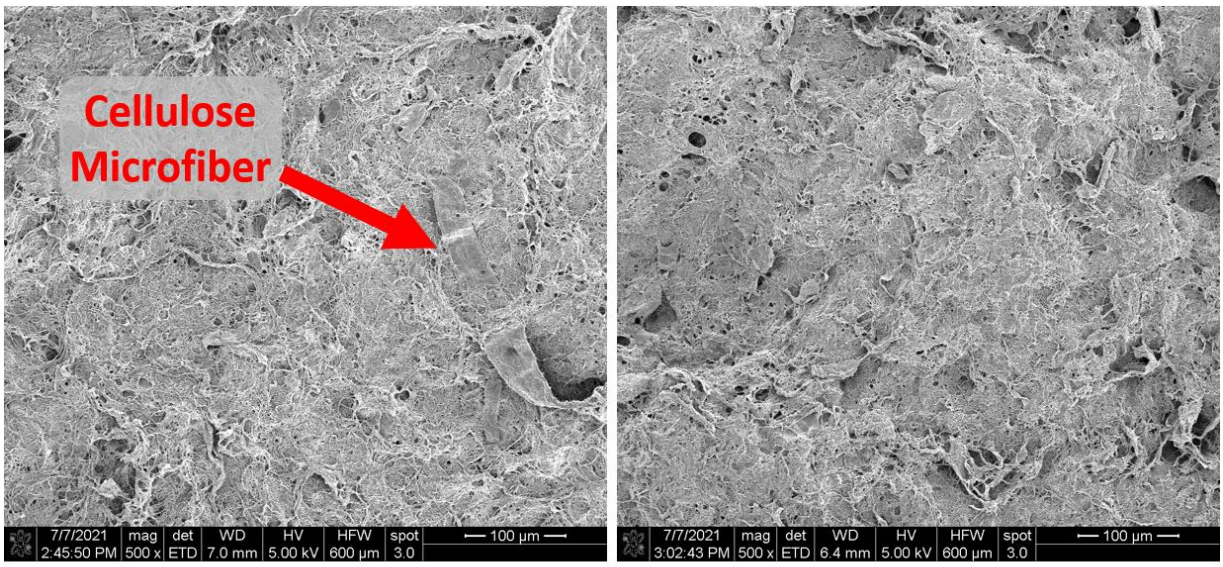

JRW 1-7a, eCNF, **90% Refined** JRW 1-7e, eCNF, **100% Refined**

Figure 2.3. SEM images of "90% refined" and "100% refined" oleyl-CNF, with the former showing the presence of microfibers.

Although structural differences in CNF refinement can be identified by SEM, subsequent studies show that they have no discernable effect on either DOS or SHP properties (to be discussed in Chapter 3). DOS data for oleyl-CNF samples prepared from 90% and 100%-refined CNFs indicate no significant differences in surface functionalization. This means previous data collected with SHP materials made from 90%-refined CNFs remain relevant and comparable to data collected from SHP materials prepared from 100%-refined CNFs.

Table 2.5. DOS and CA values of eCNFs prepared from CNFs with different refinement levels.

Sample ID	CNF Refinement	DOS	CA
JRW 1-6b	90%	0.123	161°
JRW 1-7a	90%	0.154	159°
JRW 1-24a	90%	0.128	146°
JRW 1-24b	90%	0.123	147°
JRW 1-24c	90%	0.171	142°
JRW 1-6a	100%	0.121	154°
JRW 1-7e	100%	0.160	153°
JRW 1-24d	100%	0.135	142°
JRW 1-24e	100%	0.161	157°
JRW 1-24f	100%	0.147	149°

CHAPTER 3. CHEMISTRIES FOR THE CROSSLINKING OF OLEYL-CELLULOSE NANOFIBERS

3.1 Why Reinforcement of Esterified CNF-based Materials is Necessary

Thin films prepared from eCNFs have mechanical properties and a tensile strength comparable to that of paper, and are easily torn and degraded. In addition, eCNF coatings are brittle and will crack when bent significantly. If eCNFs are to become sustainable alternatives to current thermoplastics for single-use applications, they will need to be able to do more than mimic the wetting properties of plastics. Methods must be developed to reinforce materials based on oleyl-CNF and other derivatives so that they can withstand physical stress without significant loss of mechanical integrity. Inspirations for designing a more robust eCNF-based material can be drawn from the rubber and plastics industries. Rubbers typically have a high density of covalent crosslinks between entangled polymer chains (Figure 3.1), bestowing greater mechanical strength and toughness[59] and increased resistance to tearing and chemical degradation.[60]

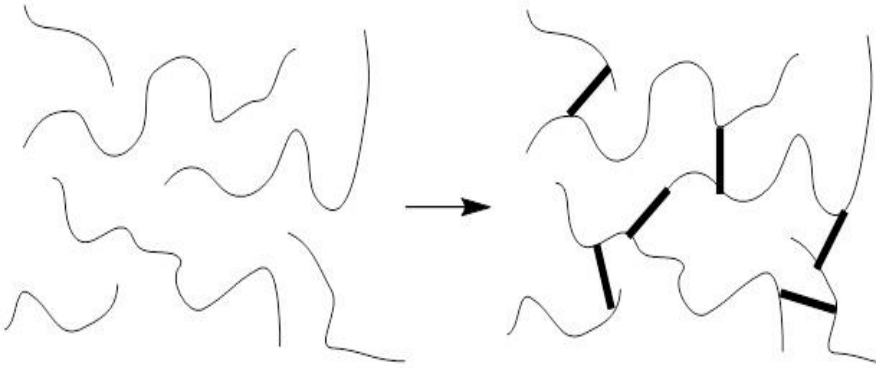

Figure 3.1. Cartoon depicting the introduction of crosslinks between free polymer chains, resulting in a covalent network.

Oleyl-CNFs have an inherent advantage over CNFs modified with saturated hydrocarbon chains because of their presentation of internal *cis*-alkenes. Alkenes can be crosslinked by several methods, as exemplified by the vulcanization of rubber[47] or by chemistries that have been vetted for use with unsaturated fatty acid chains (Figure 3.2).[50,52] Two approaches stand out for their potential to preserve the whiteness and SHP properties obtained with oleyl-CNFs: the thiol–ene "click" reaction, and alkene epoxidation followed by acid-catalyzed crosslinking with polyols.

Studies on the feasibility of these approaches will be presented in Sections 3.3 and Section 3.4, respectively.

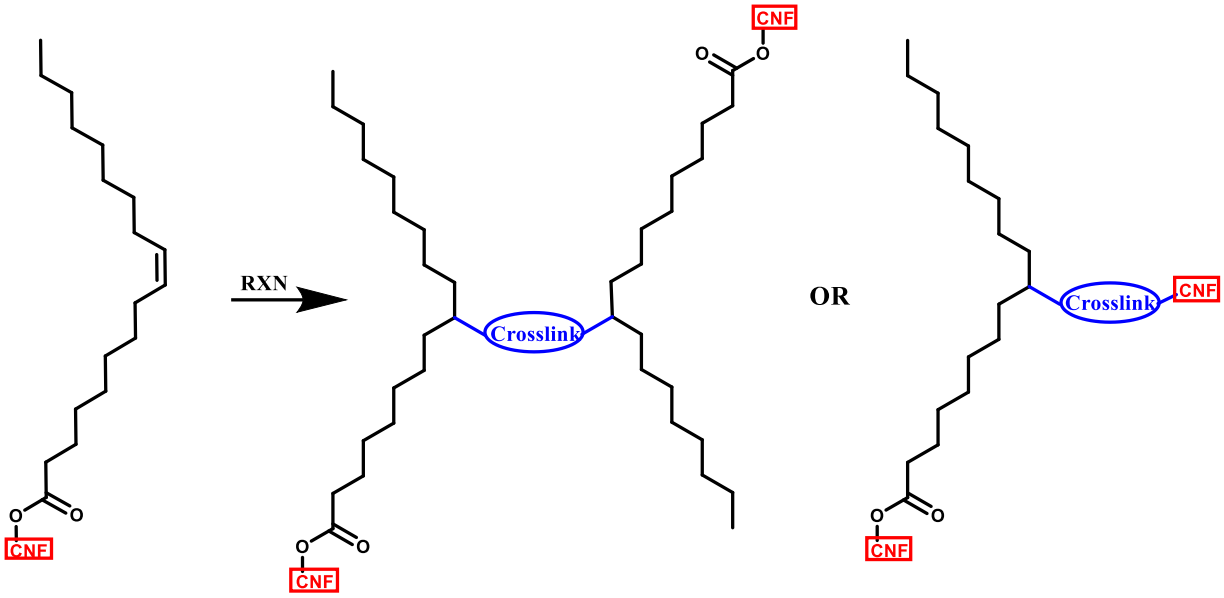

Figure 3.2. Crosslinks between two oleyl side chains or an oleyl side chain with CNF hydroxyls.

3.2 Development of Crosslinking Chemistry with Methyl Oleate

As discussed in Chapter 2, the preparation of eCNFs on a gram scale can take several days. Moreover, they are difficult to analyze spectroscopically due to their size, low solubility, and high degree of structural variance. For example, solid-state NMR of eCNFs are complex and hard to interpret if subtle covalent changes have been made. This presents a challenge for the chemical characterization of crosslinked eCNF materials, not only in terms of quantifying degree of crosslinking, but also for determining any progress of a given reaction. Of course, if crosslinking is robust then the effect on mechanical properties will become apparent, but it is far more difficult to evaluate a reaction that does not proceed efficiently. To circumvent this problem, crosslinking reactions can be evaluated first with methyl oleate, a molecular analog of oleyl-CNF (Figure 3.3). It can be reasonably assumed that if a reaction does not work on methyl oleate, it will also not work on oleyl-CNFs. Conversely, if a transformation works on methyl oleate, it is reasonable to believe that the same transformation has potential to work on oleyl-CNF. For this reason, all reactions discussed in this section have been attempted with methyl oleate and, if successful, extended to oleyl-CNF.

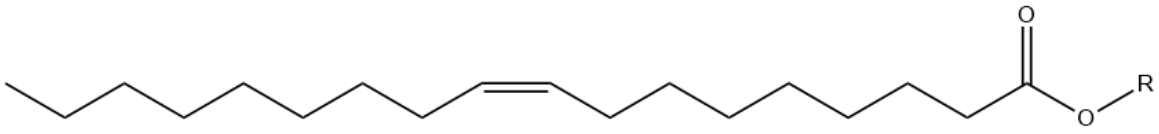

Figure 3.3. Side chain for methyl oleate (R = CH_3) and oleyl-CNF.

One limitation encountered while exploring this crosslinking chemistry was the difficulty in redispersing eCNFs that had already been fully dried. Typically, mechanical grinding of properly lyophilized CNF enables its facile dispersion during mechanochemistry, such that CNF functionalization is relatively homogenous. However, once an eCNF sample is dried— whether previously worked up or dispersed in chloroform, ethyl acetate, or ethanol— the eCNF fibers are virtually impossible to redisperse (Figure 3.4A). Attempts to use grinding or ball milling in the presence of various solvents could reduce eCNF chunks into smaller pieces, but were unsuccessful at re-establishing the homogenous suspensions that were obtained prior to drying. For this reason, it is necessary to avoid drying when further crosslinking is desired; samples should only be dried for DOS analysis or for testing SHP properties.

Figure 3.4. (A) Oleyl-CNF after mechanical grinding, demonstrating the difficulty of pulverizing dry samples. (B) Oleyl-CNF stored as a slurry in EtOH.

Fortunately, eCNF can form stable suspensions in various solvents and does not appear to suffer from degradation or agglomeration even after several weeks of storage while dispersed in ethanol, ethyl acetate, or chloroform.[4] eCNF samples need only to be stored as a slurry in

minumum EtOH or EtOAc to ensure their utility in future crosslinking reactions (Figure 3.4B). For this reason, crosslinking chemistry should be designed to be compatible with one of these solvents.

3.3 Dithiols in Thiol-Ene "Click" Chemistry

While a number of thiol-ene transformations have been reported in the literature,[54] one specific reaction condition stands out for its simplicity and proven success in the synthesis of macromolecules.[53] Koyama and coworkers reported conditions based on a radical mechanism for coupling terminal dialkenes with dithiols, using AIBN as a thermal initiator. These two reactants can form polymers with molecular weights in excess of 50,000 g/mol. The use of a thermal initiator is attractive, rather than a photoinitiator which is more common in the literature but would be hindered by the opacity of eCNF films. We reasoned that internal alkenes, such as those present in the oleate moiety, would also react to the extent that they could form crosslinks between oleyl units. For this method to work with oleyl-CNFs, a sufficiently large dithiol or polythiol would be needed to react with oleate groups attached to different nanofibers. The covalent crosslinking of eCNF fibers through their oleate groups should then augment the film's mechanical properties.

The procedure outlined by Koyama was tested with methyl oleate and dodecanethiol or 6-mercapto-1-hexanol (Figure 3.5), with the expectation of observing thiol-ene addition. Unfortunately, despite several attempts and a dedicated effort to prevent air contamination (which can quench radical reactions), NMR yields higher than 10% could not be achieved. Since eCNFs in thin-film form would likely be less reactive than methyl oleate, it was decided that this route to crosslinking was unlikely to bear fruit and was thus abandoned.

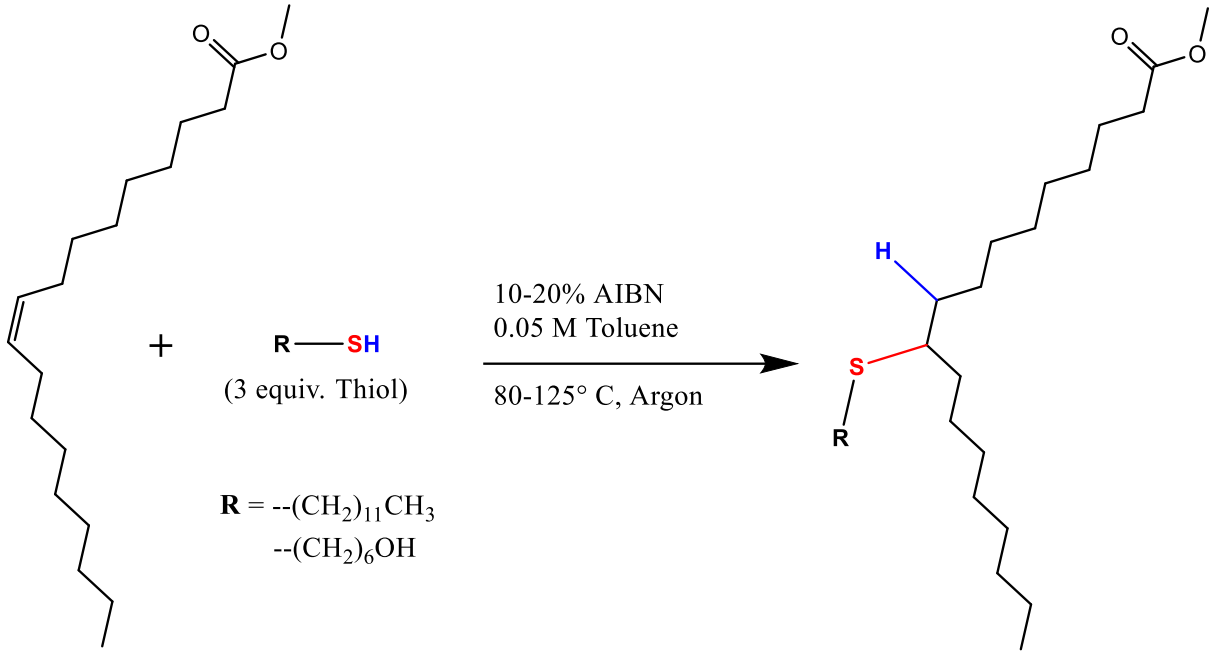

Figure 3.5. AIBN-mediated addition of thiols to methyl oleate (thiol-ene reaction).[53]

3.4 Epoxide Ring Opening for Crosslinking of Oleyl CNF

Epoxide ring-opening reactions are often used in polymerizations and crosslinking chemistries.[61-64] Epoxides are highly strained rings, making nucleophilic additions thermodynamically favorable.[65] Epoxides can be activated by the addition of a mild acid, which will produce an alcohol following nucleophilic substitution.[66] The ease with which epoxides participate in acid-catalyzed additions makes them very useful as synthetic intermediates. One possible way to create covalent crosslinks between oleyl-CNF fibers is to convert the alkenes in oleate groups into epoxides, followed by treatment with a mild acid to promote crosslinking with surface hydroxyl groups on neighboring CNF fibers. Several methods of epoxidation were tested on methyl oleate, as well as oleyl-CNF itself (Figure 3.6). We first evaluated *m*-chloroperoxybenzoic acid (mCPBA), a classic reagent used in epoxidations. Reactions were performed in DCM at reflux for 30 minutes, which resulted in the complete consumption of methyl oleate and the appearance of a new ^{1}H NMR peak around 2.9 ppm correlating to the presence of an epoxide (Figure 3.7). This reaction was then applied to methyl oleate on a horizontal ball mill without solvent or heat (Figure 3.6, Path 1); methyl epoxyoleate could be obtained in isolated yields up to 89%.

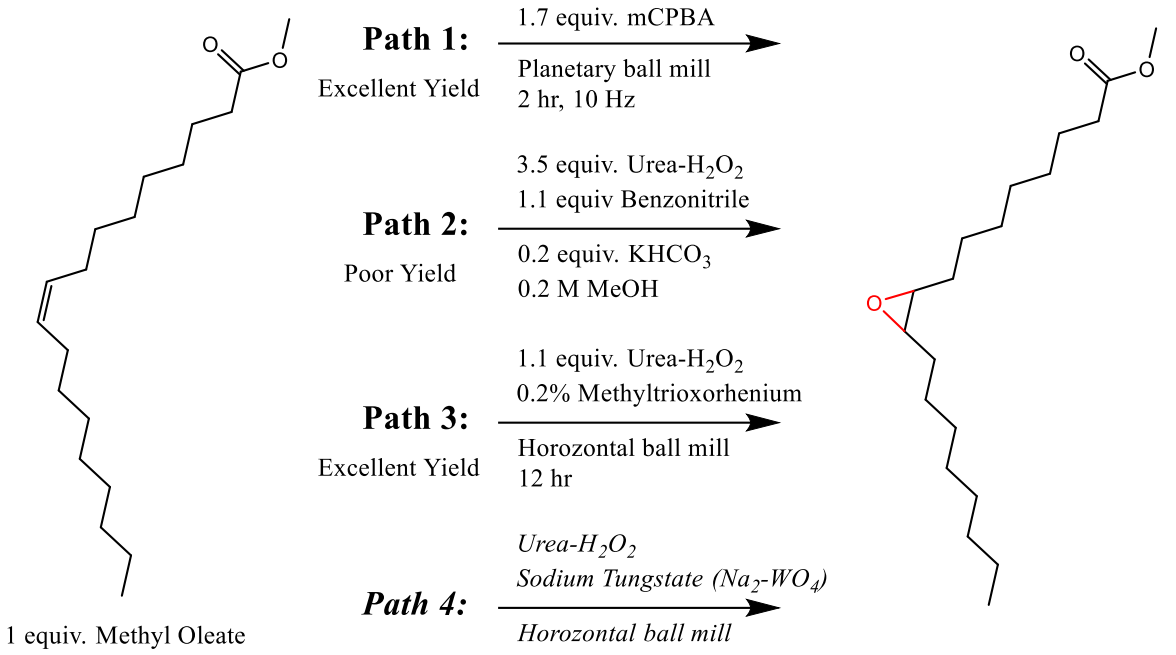

Figure 3.6. Various reactions attempted (Paths 1–3) and proposed reaction (Path 4) for the epoxidation of methyl oleate, a molecular analog of oleyl-CNF.

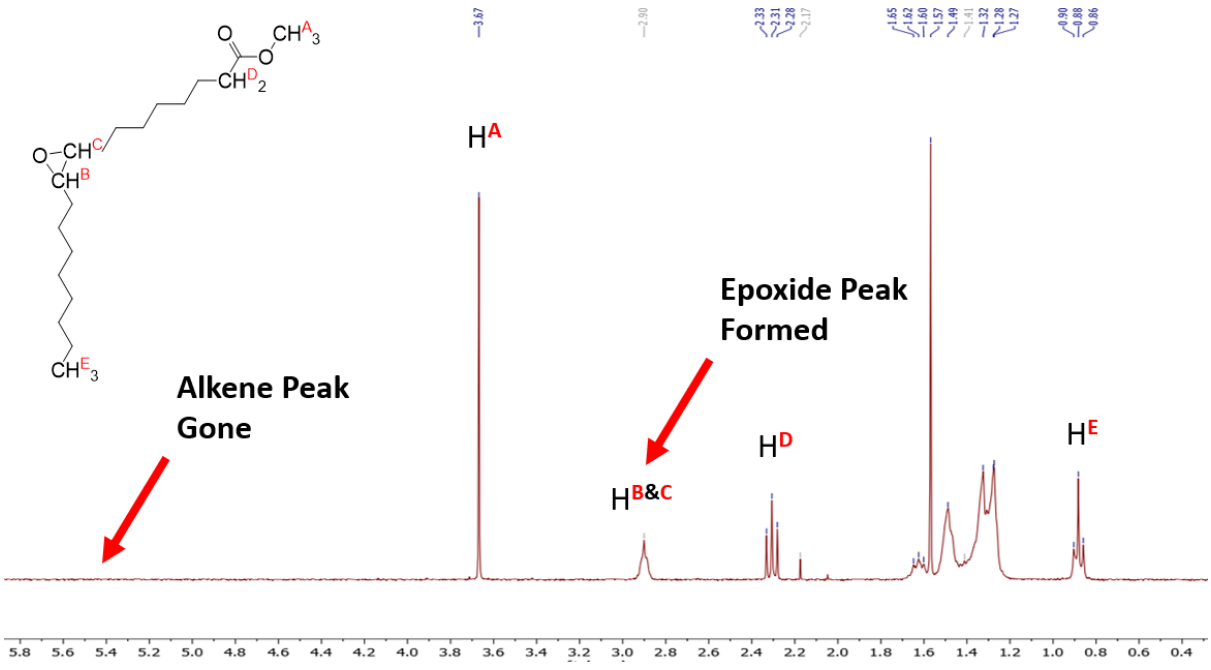

Figure 3.7. ^{1}H NMR of methyl epoxyoleate (400 MHz, $CDCl_3$).

Although the mCPBA reaction was successful, the reagent is not ideal for use in an allegedly "green" process as mCPBA is known to be unstable and can combust spontaneously if

mishandled. This issue is at odds with Tenet #12 in the Principles of Green Chemistry discussed in the introduction. Even when used correctly, mCPBA produces significant waste (*m*-chlorobenzoic acid) when used in large quantities. Given this reaction produces an unfavorable byproduct (Tenet #1) and suffers from poor atom economy (Tenet #2), a greener alternative was desirable.

Urea–H_2O_2 (UHP) is a much greener oxygen transfer agent than mCPBA or other organic peroxides. UHP is a complex stabilized by hydrogen bonding between urea, a naturally occurring and environmentally mild chemical, and H_2O_2 (Figure 3.8). Unlike concentrated H_2O_2, UHP exists as an air-stable solid that is well suited for long-term storage. UHP is prepared simply by dissolving urea in 30% aqueous H_2O_2 in a 2:3 molar ratio at 60 °C, then cooling the solution until UHP precipitates in crystalline form.[67] UHP readily dissociates in water into free urea and H_2O_2 but is less reactive than mCPBA or other peroxides. Specifically, simply replacing mCPBA with UHP in the ball-milling procedure described above did not result in epoxidation of methyl oleate.

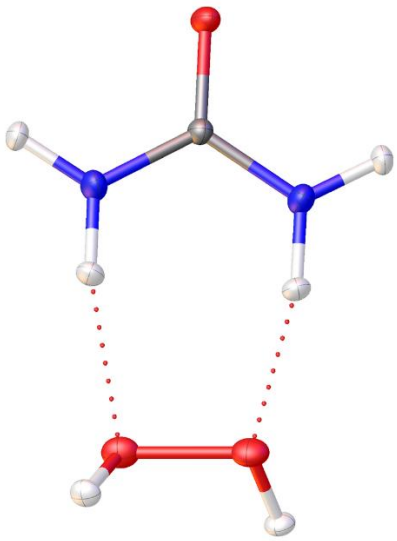

Figure 3.8. Crystal structure of the urea–hydrogen peroxide (UHP) complex.[73]

Several alkene epoxidations using UHP have been reported, some in combination with a catalyst and others performed in metal-free conditions.[68-72] A good example of the latter involves the use of benzonitrile to promote UHP peroxidation (Figure 3.6, Path 2). This reaction uses several equivalents of both benzonitrile and UHP (which lowers its apparent atom economy), however the

authors claim that the reaction byproducts (urea and benzamide) can be extracted and upcycled. Regardless, this method stands out for its metal-free and relatively mild conditions. Unfortunately, epoxidation of methyl oleate by this approach never exceeded 10%, despite numerous attempts.

We then evaluated methyltrioxorhenium (MTO)-catalyzed UHP epoxidation, which has been used with great success by several research groups.[70,72] Methyl oleate in TBA was treated with several equivalents of UHP and 1 mol% MTO, heated to reflux for 3 hours, and was converted quantitatively into an epoxide based on NMR analysis. This motivated us to develop conditions for MTO-catalyzed UHP epoxidation using solventless ball milling. Ultimately, we determined that MTO-catalyzed UHP epoxidation of methyl oleate could proceed efficiently under ball-milling conditions with a stoichiometric amount of UHP and 0.2 wt% MTO, at room temperature and without added solvent (Figure 3.6, Path 3). A detailed procedure is presented below:

Epoxidation:

- Add 11 zirconia balls (10-mm diameter) to a 100-mL Nalgene bottle.
- Add 0.500 g methyl oleate, 0.174 g UHP, and 1.0 mg MTO.
- Place on horizontal ball mill for 12 hours at 350 rpm.

Workup:

- Dilute reaction slurry with ether, then filter through washed Celite.
- In a separatory funnel, wash twice with 5% aq. $NaHSO_3$ and once with H_2O.
- Dry organic phase with Na_2SO_4, then condense by rotary evaporation.

The ^1H NMR spectrum of the reaction product indicated the absence of alkene protons associated with methyl oleate, and the appearance of a new peak at 2.9 ppm corresponding to an epoxide (Figure 3.9). The methyl epoxyoleate could be purified by silica gel chromatography with isolated yields as high as 85%. We also determined that the MTO-catalyzed epoxidation was unaffected by the presence of ethanol or ethyl acetate. This is an important practical factor as oleyl-CNF is maintained as a damp slurry in these solvents, as discussed in Section 3.2.

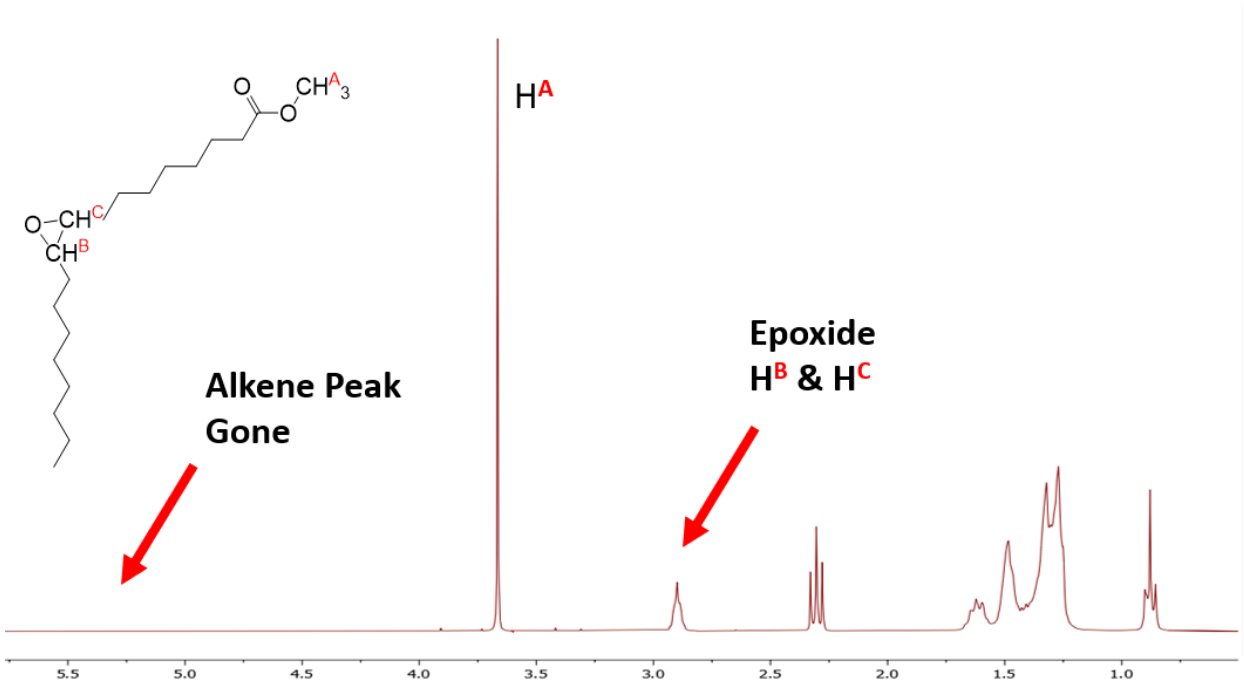

Figure 3.9. ^{1}H NMR (400 MHz, $CDCl_3$) of methyl epoxyoleate synthesized by MTO-catalyzed UHP epoxidation under mechanochemical conditions.

We also obtained some evidence that mechanochemical MTO-catalyzed epoxidation also works with oleyl-CNF, however spectroscopic evidence has proven ambiguous. The alkene C–H peak in the FT-IR spectrum of oleyl-CNF is weak, and C–O stretching modes corresponding to the epoxide are buried deeply within the fingerprint region amidst other C–O stretching modes from cellulose. Solid-state NMR is challenging to arrange and unlikely to be informative, based on the quality of spectra for eCNFs by previous lab members. We thus considered qualitative methods of chemical analysis to evaluate the presence of epoxides.

One method previously reported as a TLC-based test for epoxides involves a picric acid stain, which produces a faint orange color against a yellow background.[74] While the subtle difference in color may be sufficient for TLC analysis, the stain unfortunately did not provide sufficient indication of epoxidation on substrates prepared from modified CNFs.

On the other hand, we were able to observe a qualitative change in the physical properties of the epoxidized oleyl-CNFs upon drying. While films of oleyl-CNF can be considered superhydrophobic (CA >160°), the films and surfaces of epoxidized oleyl-CNF are clearly hydrophilic (CA <90°). The large increase in wettability suggests a chemical change, namely functional groups with greater polarity, which would be consistent with epoxidation. While not

definitive evidence, this observation is sufficient to motivate additional efforts in product characterization.

For crosslinking, we have been exploring acid-catalyzed epoxide ring opening reactions with a diol. For example, methyl epoxyoleate was mixed with diethylene glycol in the presence of *p*-toluenesulfonic acid (TsOH), which has a pK_a of –2.8.[75] Such reactions are highly sensitive to water, which is a more reactive nucleophile under acidic conditions than higher molecular weight hydroxyls or cellulose, and requires careful drying of reagents and starting materials. Research on this reaction remains in progress.

CHAPTER 4. SPRAY COATING APPLICATIONS OF OLEYL CNF MATERIALS

4.1 Optimization of Spray-coating Procedure

In order to spray-coat eCNFs, the material has to be dispersed in a volatile solvent. Dr. Miran Malvan has previously observed eCNF materials to form stable suspensions in several organic solvents.[4] Chief among these was chloroform, which produced visibly stable dispersions after the course of several days. In fact, suspensions for spray coating do not need to remain stable for more than a few hours. For this reason, we explored additional organic solvents with greater potential for green processes.[56] We found that ethyl acetate could also be used to prepare oleyl-CNF suspensions that are sufficiently stable for spray-coating applications.

EtOAc suspensions can be prepared using "wet" oleyl-CNF stored with minimal EtOH (see Section 3.2 and Figure 3.4B). In a standard procedure, 10 g of ethanolic eCNF slurry is mixed vigorously with 40 mL EtOAc until homogenous. This suspension can be sprayed using a commercially available airbrush (Figure 4.1), positioned 6 inches away from the surface in slow, even strokes, with pauses for solvent evaporation between coats. Multiple layers can be applied in this way until the desired coverage is achieved, which is typically 10–20 layers. The final coatings are quite thin due to the level of dilution and even after 20 coats the added mass and thickness of the coating is minute.

Figure 4.1. Commercially available airbrush used for eCNF spray coating.

Oleyl-CNF coatings can be applied onto a range of materials, including cardboard, aluminum, glass, polystyrene, and others. These coatings adhere to surfaces without visible peeling or cracks, and the topmost layer can be exfoliated by mild abrasion. This last feature can preserve and even enhance the superhydrophobic character of the oleyl-CNF coating, as established by static contact angle measurements and sliding angles (Table 4.1). As previously demonstrated with oleyl-CNF wafers prepared by simple filtration and drying,[4] the SHP properties of spray-coated oleyl-CNF can be lost by surface fouling, but restored by exfoliation methods such as delamination with an adhesive tape. We have found that "Scotch-tape" exfoliation can be performed over a dozen times without ruining the integrity of the SHP coating.

Table 4.1. Static contact angle and sliding angles of oleyl-CNF coatings on various substrates

Sample	Static Contact Angle	Sliding Angle
Glass	163°	5°
Aluminum	161°	5°
Cardboard	159°	5°
Polystyrene	164°	5°
Dirty	126°	--
Exfoliated (x12)	161°	5°

4.2 Applications of Spray-coated Oleyl-CNF

The ability to imbue objects with a cheap, green, and superhydrophobic coating can potentially provide exciting opportunities for many industries. For instance, carboard and paper packages could be made resistant to rain and moisture if coated with a superhydrophobic layer of oleyl-CNF. Several examples of objects spray-coated with oleyl-CNF can be seen in this section. In one case, a cardboard box coated with oleyl-CNF remains dry while floating on the surface of a tub of water until forced down, at which point water begins to seep in between the seams (Figure 4.2). In a second example, a piece of paper was sprayed in the center with oleyl-CNF then subjected to laser printing without smearing; the treated paper remained non-wetting in the area that oleyl-CNF had been applied (Figure 4.3). These examples demonstrate the possibility of printing labels and logos onto surfaces already coated with oleyl-CNF, with retention of its SHP properties. Lastly, a piece of newspaper was spray-coated on both sides with oleyl-CNF, then folded by origami into

a paper boat that could float for hours on water without loss of structural integrity, unlike an untreated newspaper boat that wetted instantly and sank within minutes (Figure 4.4).

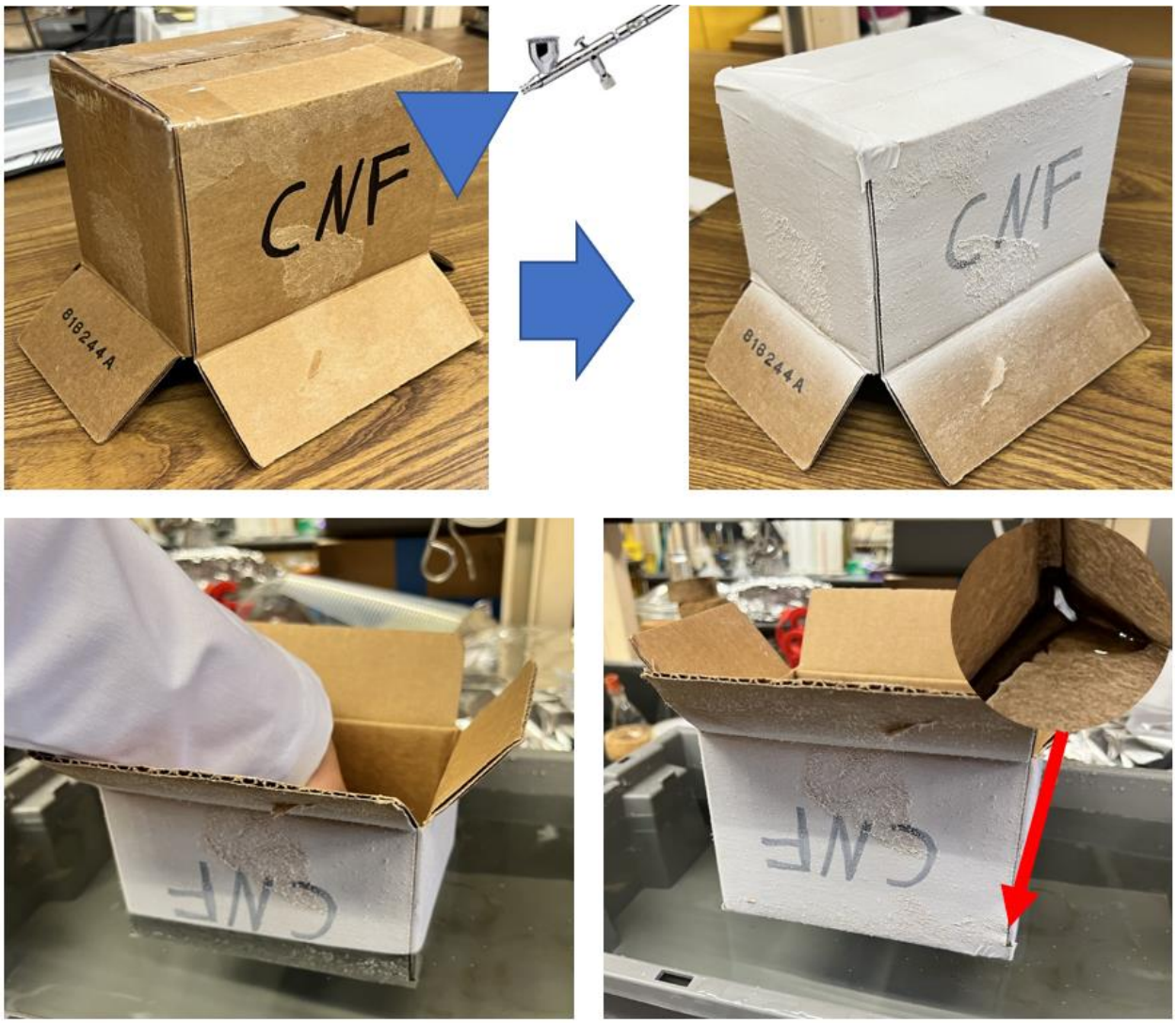

Figure 4.2. A cardboard box sprayed with oleyl-CNF becomes non-wetting on the outer surfaces, although forced submersion in water leads to leakage through the seams.

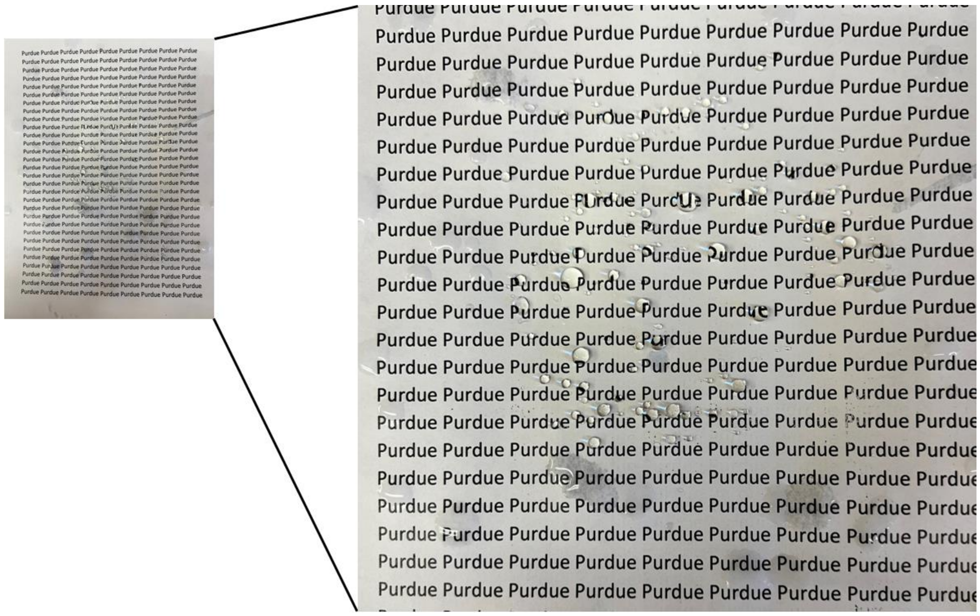

Figure 4.3. Printer paper sprayed in the center with oleyl CNF can still be printed on and will maintain its non-wetting character.

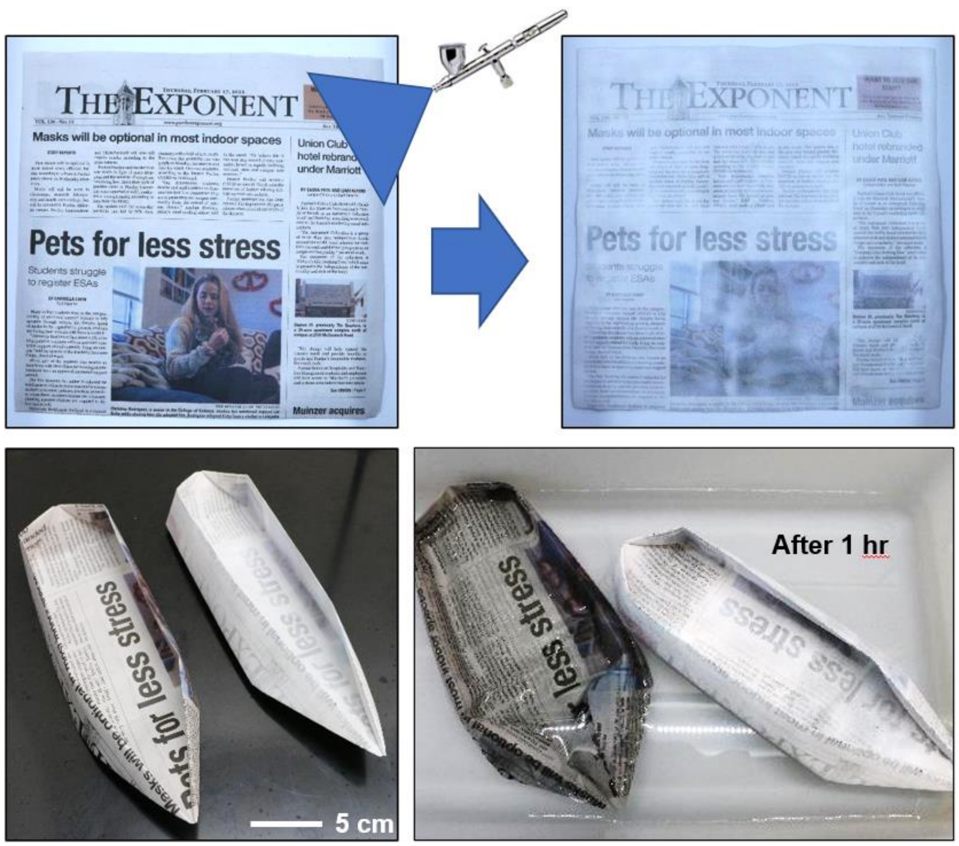

Figure 4.4. Newspaper spray-coated with Oleyl-CNF can be folded into an origami boat that is non-wetting and remains afloat even after several hours.

CONCLUSION

Cellulose nanofibrils present exciting opportunities for biorenewable materials, especially when modified with fatty acids through mechanochemical esterification. The synthesis of esterified CNFs is potentially scalable to kilogram quantities, and optimizations in protocol have enabled its production time to be reduced to just three days using low-energy methods for purification. Oleyl-CNF coatings have demonstrated unique anti-wettability properties and can repel water strongly enough to qualify as superhydrophobic, which appears to be an innate feature of the oleyl-CNFs themselves. Furthermore, oleyl-CNF can be dispersed in ethyl acetate and deposited onto a variety of surfaces using a standard airbrush, imbuing a diverse array of materials with restorable superhydrophobic properties. Methods to chemically reinforce oleyl-CNF via covalent crosslinking have been investigated, with mechanochemical epoxidation showing great promise. This sets the stage for future efforts to develop the crosslinking chemistry, as well as to investigate the biodegradability of eCNF materials in as-deposited and crosslinked forms.

REFERENCES

[1] Yale. (2017). *History of Green Chemistry. Center for Green Chemistry & Green Engineering at Yale*. Retrieved March 14, 2022, from https://greenchemistry.yale.edu/about/history-green-chemistry.

[2] Anastas, P. T.; Warner, J. C. (1998) *Green Chemistry: Theory and Practice,* Oxford University Press: New York, p.30.

[3] Beach, E. S.; Cui, Z.; Anastas P. T. Green Chemistry: A design framework for sustainability. *Energy Environmental Science.*, **2009**, *2*, 1038-1049.

[4] Malvan, M. (2019). *Engineering Cellulose Nanofibers For Better Performance As Nanocomposites And Its Implications For Advanced Materials*. Ph.D. thesis, Department of Chemistry, West Lafayette.

[5] Cellulose. In *Kirk-Othmer Encyclopedia of Chemical Technology*.

[6] Dai, D.; Fan, M.; Collins, P., Fabrication of nanocelluloses from hemp fibers and their application for the reinforcement of hemp fibers. *Industrial Crops and Products* **2013**, *44*, 192-199.

[7] Klemm, D.; Schumann, D.; Udhardt, U.; Marsch, S., Bacterial synthesized cellulose — artificial blood vessels for microsurgery. *Progress in Polymer Science* **2001**, 26, 1561-1603.

[8] Sano, M. B.; Rojas, A. D.; Gatenholm, P.; Davalos, R. V., Electromagnetically controlled biological assembly of aligned bacterial cellulose nanofibers. *Annals of Biomedical Engineering* **2010**, 38, 2475-84.

[9] Feng, X.; Ullah, N.; Wang, X.; Sun, X.; Li, C.; Bai, Y.; Chen, L.; Li, Z., Characterization of Bacterial Cellulose by *Gluconacetobacter hansenii* CGMCC 3917. *Journal of Food Science* **2015**, 80, E2217-27.

[10] Moniri, M.; Boroumand Moghaddam, A.; Azizi, S.; Abdul Rahim, R.; Bin Ariff, A.; Zuhainis Saad, W.; Navaderi, M.; Mohamad, R., Production and Status of Bacterial Cellulose in Biomedical Engineering. *Nanomaterials* **2017**, *7*, 257.

[11] Zhao, Y.; Li, J. J. C., Excellent chemical and material cellulose from tunicates: diversity in cellulose production yield and chemical and morphological structures from different tunicate species. *Cellulose* **2014**, *21*, 3427-3441.

[12] Pettersen, R. C. (1984). The chemical composition of wood. In *The Chemistry of Solid Wood*, 57-126. ACS Advances in Chemistry.

[13] Jose Chirayil, C.; Mathew, L.; Thomas, S., Review of recent research in nano cellulose preparation from different lignocellulosic fibers. *Reviews on Advanced Materials Science* **2014**, *37*, 20-28.

[14] George, J.; Sabapathi, S. N., Cellulose nanocrystals: synthesis, functional properties, and applications. *Nanotechnology, Science and Applications* **2015**, *8*, 45-54.

[15] Filson, P. B.; Dawson-Andoh, B. E.; Schwegler-Berry, D., Enzymatic-mediated production of cellulose nanocrystals from recycled pulp. *Green Chemistry* **2009**, *11*, 1808-1814.

[16] Lu, P.; Hsieh, Y.-L., Preparation and properties of cellulose nanocrystals: Rods, spheres, and network. *Carbohydrate Polymers* **2010**, *82*, 329-336.

[17] Xu, X.; Liu, F.; Jiang, L.; Zhu, J. Y.; Haagenson, D.; Wiesenborn, D. P., Cellulose Nanocrystals vs. Cellulose Nanofibrils: A Comparative Study on Their Microstructures and Effects as Polymer Reinforcing Agents. *ACS Applied Materials & Interfaces* **2013**, *5*, 2999-3009.

[18] The Biosynthesis of Cellulose AU - Brown, R. Malcolm. *Journal of Macromolecular Science, Part A* **1996**, *33*, 1345-1373.

[19] Nogi, M.; Iwamoto, S.; Nakagaito, A. N.; Yano, H., Optically Transparent Nanofiber Paper. *Advanced Materials* **2009**, *21*, 1595-1598.

[20] Peng, S. X.; Chang, H.; Kumar, S.; Moon, R. J.; Youngblood, J. P., A comparative guide to controlled hydrophobization of cellulose nanocrystals via surface esterification. *Cellulose* **2016**, *23*, 1825-1846.

[21] Yoo, Y.; Youngblood, J. P., Green One-Pot Synthesis of Surface Hydrophobized Cellulose Nanocrystals in Aqueous Medium. *ACS Sustainable Chemistry & Engineering* **2016**, *4*, 3927-3938.

[22] Yano, H.; Omura, H.; Honma, Y.; Okumura, H.; Sano, H.; Nakatsubo, F., Designing cellulose nanofiber surface for high density polyethylene reinforcement. *Cellulose* **2018**, *25*, 3351-3362.

[23] Wang, T.; Drzal, L. T., Cellulose-Nanofiber-Reinforced Poly(lactic acid) Composites Prepared by a Water-Based Approach. *ACS Applied Materials & Interfaces* **2012**, *4*, 5079-5085.

[24] Chen, C.; Mo, M.; Chen, W.; Pan, M.; Xu, Z.; Wang, H.; Li, D., Highly conductive nanocomposites based on cellulose nanofiber networks via NaOH treatments. *Composites Science and Technology* **2018**, *156*, 103-108.

[25] Raymond, M. J.; Slater, C. S.; Savelski, M. J. LCA approach to the analysis of solvent waste issues in the pharmaceutical industry. *Green Chem.*, **2010**, *12*, 1826-1834.

[26] Takacs, L., The historical development of mechanochemistry. *Chemical Society Reviews* **2013**, *42*, 7649-7659.

[27] Takacs, L., The Father of Mechanochemistry. *Bulletin for the History of Chemistry* **2004**, *28*, 26-34.

[28] Hernández, J. G.; Bolm, C., Altering Product Selectivity by Mechanochemistry. *The Journal of Organic Chemistry* **2017**, *82*, 4007-4019.

[29] Do, J.-L.; Friščić, T., Mechanochemistry: A Force of Synthesis. *ACS Central Science* **2017**, *3*, 13-19.

[30] Thiessen, P. A. M., K.; Heinicke, G., Grundlagen Der Tribochemie. *Materials and Corrosion,* **1967,** *19*, 188-189.

[31] Kang, X.; Sun, P.; Kuga, S.; Wang, C.; Zhao, Y.; Wu, M.; Huang, Y. Thin Cellulose Nanofiber from Corncob Cellulose and Its Performance in Transparent Nanopaper. *ACS Sustainable Chemical Engineering* **2017**, *5*, 2529–2534.

[32] Fernandes Diniz, J. M. B.; Gil, H.; Castro, J. A. A. M., Hornification—its origin and interpretation in wood pulps. *Wood Science and Technology* **2004**, *37*, 489-494.

[33] Elazzouzi-Hafraoui, S.; Nishiyama, Y.; Putaux, J.-L.; Heux, L.; Dubreuil, F.; Rochas, C., The Shape and Size Distribution of Crystalline Nanoparticles Prepared by Acid Hydrolysis of Native Cellulose. *Biomacromolecules* **2008**, *9*, 57-65.

[34] Huang, P.; Wu, M.; Kuga, S.; Wang, D.; Wu, D.; Huang, Y., One-Step Dispersion of Cellulose Nanofibers by Mechanochemical Esterification in an Organic Solvent. *ChemSusChem* **2012**, *5*, 2319-2322.

[35] Buckton, G., Contact angle, adsorption and wettability — A review with respect to powders. *Powder Technology* **1990**, *61*, 237-249.

[36] Bormashenko, E.; Gendelman, O.; Whyman, G., Superhydrophobicity of Lotus Leaves versus Birds Wings: Different Physical Mechanisms Leading to Similar Phenomena. *Langmuir* **2012**, *28*, 14992-14997.

[37] Huhtamäki, T.; Tian, X.; Korhonen, J. T.; Ras, R. H. A., Surface-wetting characterization using contact-angle measurements. *Nature Protocols* **2018**, *13*, 1521-1538.

[38] Xue, X.; Yang, Z.; Li, Y.; Sun, P.; Feng, Y.; He, Z.; Qu, T.; Dai, J.-G.; Zhang, T.; Qin, J.; Xu, L.; Zhang, W., Superhydrophobic self-cleaning solar reflective orange-gray paint coating. *Solar Energy Materials and Solar Cells* **2018**, *174*, 292-299.

[39] Zheng, Q.; Lü, C., Size Effects of Surface Roughness to Superhydrophobicity. *Procedia IUTAM* **2014**, *10*, 462-475.

[40] Wenzel, R. N., Resistance of Solid Surfaces to Wetting by Water. *Industrial & Engineering Chemistry* **1936**, *28*, 988-994.

[41] Song, J., Rojas O., Approaching super-hydrophobicity from cellulosic materials: A Review. *Nordic Pulp and Paper Research Journal* **2013**, *28*, 216-238.

[42] Almeida, A. P. C.; Canejo, J. P.; Fernandes, S. N.; Echeverria, C.; Almeida, P. L.; Godinho, M. H., Cellulose-Based Biomimetics and Their Applications. *Advanced Materials* **2018**, *30*, 1703655.

[43] Huang, J.; Lyu, S.; Fu, F.; Chang, H.; Wang, S., Preparation of superhydrophobic coating with excellent abrasion resistance and durability using nanofibrillated cellulose. *RSC Advances* **2016**, *6*, 106194-106200.

[44] Zheng, X.; Fu, S., Reconstructing micro/nano hierarchical structures particle with nanocellulose for superhydrophobic coatings. *Colloids and Surfaces A: Physicochemical and Engineering Aspects* **2019**, *560*, 171-179.

[45] Teisala, H.; Tuominen, M.; Kuusipalo, J., Superhydrophobic Coatings on Cellulose-Based Materials: Fabrication, Properties, and Applications. *ACS Advanced Materials and Interfaces* **2014**, *1*, 1300026.

[46] Kaushik, M.; Moores, A., Review: nanocelluloses as versatile supports for metal nanoparticles and their applications in catalysis. *Green Chemistry* **2016**, *18*, 622-637.

[47] Kato, H.; Nakatsubo, F.; Abe, K.; Yano, H. Crosslinking via sulfur vulcanization of natural rubber and cellulose nanofibers incorporating unsaturated fatty acids. *RSC Advances* **2015**, *5*, 29814.

[48] Selbes, M.; Yilmaz, O.; Khan, A. A.; Karanfil, T. Leaching of DOC, DN, and inorganic constituents from scrap tires. *Chemosphere* **2015**, *139*, 617-623.

[49] Lv, M.; Fang, L.; Yu, H.; Rojruthai, P.; Sakdapipanich, J. Discoloration Mechanisms of Natural Rubber and Its Control. *Polymers* **2022**, *14*, 764-777.

[50] Lluch, C.; Ronda, J. C.; Galia, M.; Lligadas, G.; Cadiz, V. Rapid Approach to Biobased Telechelics through Two One-Pot Thiol-Ene Click Reactions. *Biomacromolecules*, **2010** *11* 1646–1653.

[51] Ortiz, R. A.; Martinez A. Y. R.; Valdez, A. E. G.; Duarte, M. L. B. Synthesis of a novel biopolymer by means of thiol-ene photopolymerization using diallyl sucrose and dithiotreitol as comonomers. *MRS Proceedings*. **2010**, *1277*, 6-10.

[52] Gonza, R.; Lez-Paz, R.; Lluch, C.; Lligadas, G.; Ronda, J. C.; Galia, M.; Cadiz, V. Green Approach Toward Oleic- and Undecylenic Acid-Derived Polyurethanes. *Journal of Polymer Science Part A: Polymer Chemistry* **2011**, *49*, 2407–2416.

[53] Koyama E.; Sanda, F.; Endo, T. Radical Polyadditions of Dithiols with Diolefins Derived from Optically Active Amino Alcohols. *Macromolecules*, **1998**, *31*, 1495–1500.

[54] Lowe, A. B. Thiol-ene ‘‘click’’ reactions and recent applications in polymer and materials synthesis. *Polymer Chemistry* **2010**, *1*, 17–36.

[55] Berlan, J.; Mason, T. J. Sonochemistry: from research laboratories to industrial plants. *Ultrasonics* **1992**, *30*, 4, 203-212.

[56] Adler, C. M.; Hayler, J. D.; Henderson, R. K.; Redman, A. M.; Shukla, L.; Shuster, L. E.; Sneddon, H. F. Updating and further expanding GSK’s solvent sustainability guide. *Green Chemistry* **2016**, *18*, 3879-3890.

[57] Kasraian, K.; Deluca, P. P., Thermal-Analysis of the Tertiary Butyl Alcohol-Water System and Its Implications on Freeze-Drying. *Pharmaceutical Researcher* **1995**, *12*, 484-490.

[58] Searles J. A. (2010) Freeze-Drying/Lyophilization of Pharmaceutical and Biological Products. In *Freezing and Annealing Phenomena in Lyophilization*. CRC Press.

[59] Gent, A. N. (2018). *Engineering with Rubber: How to Design Rubber Components*. Hanser.

[60] Zweifel, H.; Maier, R. D.; Schiller, M. (2009). *Plastics Additives Handbook* (6th ed.). Munich: Hanser. p. 746.

[61] Burfield, D. Epoxy groups responsible for crosslinking in natural rubber. *Nature* **1974,** *249*, 29–30.

[62] Brocas, A.-L.; Mantzaridis, C.; Tunc, D.; Carlotti, S. Polyether synthesis: From activated or metal-free anionic ring-opening polymerization of epoxides to functionalization. *Progress in Polymer Science* **2013**, *38*, 845-873.

[63] Jin, F.-L.; Rhee, K. Y.; Park, S.-J. Functionalization of multi-walled carbon nanotubes by epoxide ring-opening polymerization. *Journal of Solid State Chemistry* **2011,** *184*, 3253-3256.

[64] Sarazin, Y.; Carpenter, J.-F. Discrete Cationic Complexes for Ring-Opening Polymerization Catalysis of Cyclic Esters and Epoxides. *Chemistry Reviews* **2015**, *115*, 3564–3614.

[65] Parker, R. E.; Isaacs, N. S. Mechanisms of Epoxide Reactions *Chem. Rev.* **1959**, *59*, 737–799.

[66] Tokunaga, M.; Larrow, J. F.; Kakiuchi, F.; Jacobsen, E. N. Asymmetric Catalysis with Water: Efficient Kinetic Resolution of Terminal Epoxides by Means of Catalytic Hydrolysis. *Science* **1997,** *277*, 936-938.

[67] Lu C.-S.; Hughes, E.W.; Giguère, P.A. The crystal structure of the urea-hydrogen peroxide addition compound $CO(NH_2)_2 \cdot H_2O_2$. *Journal of the American Chemical Society* **1941**, *63*, 1507–1513.

[68] Fan, C. L.; Lee, W.-D.; Teng, N.-W.; Sun, Y.-C.; Chen, K. Epoxidation of Chiral Camphor *N*-Enoylpyrazolidinones with Methyl(trifluoromethyl)dioxirane and Urea Hydrogen Peroxide/Acid Anhydride: Reversal of Stereoselectivity. *Journal of Organic Chemistry* **2003**, *68*, 9816-9818.

[69] Ji, L.; Wang, Y.-N.; Qian, C.; Chen, X.-Z. Nitrile-Promoted Alkene Epoxidation with Urea–Hydrogen Peroxide (UHP). *Synthetic Commun*ications **2013**, *43*, 2256-2264.

[70] Sica, D. CH_3ReO_3-catalyzed oxidation of cholesta-5,7-dien-3β-yl acetate with the urea-hydrogen peroxide adduct under various conditions. Synthesis of the natural epoxy sterol 9α,11α-epoxy-5α-cholest-7-en-3β,5,6β-triol. *Steroids* **2002**, *67*, 661-668.

[71] Xu, Y.; Khaw, N. R. B. J.; Li, Z. Efficient epoxidation of alkenes with hydrogen peroxide, lactone, and lipase. *Green Chem.*, **2009**, *11*, 2047-2051.

[72] Fenelli, S. P.; Schultz, R. A. (1996). Methyltrioxorhenium-urea hydrogen peroxide epoxidation of olefins (U.S. Patent No. 5,723,636A). U.S. Patent and Trademark Office.

[73] Hydrogen peroxide – urea. (2022, March 3). In *Wikipedia*. https://en.wikipedia.org/wiki/Hydrogen_peroxide_-_urea.

[74] Fioriti, J. A.; Bentz, A. P.; Sims, R. J. The reaction of picric acid with epoxides. II. The detection of epoxides in heated oils. *Journal of the American Oil Chemists' Society* **1966,** *43*, 487-90.

[75] Guthrie, J. P. Hydrolysis of esters of oxy acids: pK_a values for strong acids. *Canadian Journal of Chemistry* **1978**, *56*, 2342-2354.